AVRADCOM
Report No. TR 81-F-9

AD

MANUFACTURING METHODS AND TECHNOLOGY
(MANTECH) PROGRAM

DEVELOPMENT OF MANUFACTURING TECHNOLOGY FOR FABRICATION OF A COMPOSITE HELICOPTER MAIN ROTOR SPAR BY TUBULAR BRAIDING

MARK L. WHITE
Kaman Aerospace Corporation
Old Windsor Road
Bloomfield, Connecticut 06002

April 1981

FINAL REPORT

Contract No. DAAG46-78-C-0070

U.S. ARMY AVIATION RESEARCH AND DEVELOPMENT COMMAND

The findings in this report are not to be construed as an official Department of the Army position, unless so designated by other authorized documents.

Mention of any trade names or manufacturers in this report shall not be construed as advertising nor as an official indorsement or approval of such products or companies by the United States Government.

DISPOSITION INSTRUCTIONS

Destroy this report when it is no longer needed.
Do not return it to the originator.

UNCLASSIFIED

SECURITY CLASSIFICATION OF THIS PAGE (When Data Entered)

REPORT DOCUMENTATION PAGE	READ INSTRUCTIONS BEFORE COMPLETING FORM
1. REPORT NUMBER: AVRADCOM TR 81-F-9 — 2. GOVT ACCESSION NO.: AD-A109 377	3. RECIPIENT'S CATALOG NUMBER:
4. TITLE (and Subtitle): DEVELOPMENT OF MANUFACTURING TECHNOLOGY FOR FABRICATION OF A COMPOSITE HELICOPTER MAIN ROTOR SPAR BY TUBULAR BRAIDING	5. TYPE OF REPORT & PERIOD COVERED: Final - Sep 78 to Sep 80
	6. PERFORMING ORG. REPORT NUMBER: R-1618
7. AUTHOR(s): Mark L. White	8. CONTRACT OR GRANT NUMBER(s): DAAG46-78-C-0070
9. PERFORMING ORGANIZATION NAME AND ADDRESS: Kaman Aerospace Corporation, Old Windsor Road, Bloomfield, Connecticut 06002	10. PROGRAM ELEMENT, PROJECT, TASK AREA & WORK UNIT NUMBERS: D/A Project: 1767079; AMCMS Code: 1497946S7079 (XS6)
11. CONTROLLING OFFICE NAME AND ADDRESS: US Army Aviation Research and Development Command, ATTN: DRDAV-EGX, 4300 Goodfellow Blvd., St. Louis, Missouri 63120	12. REPORT DATE: April 1981
	13. NUMBER OF PAGES: 77
14. MONITORING AGENCY NAME & ADDRESS (if different from Controlling Office): Army Materials and Mechanics Research Center, ATTN: DRXMR-AP, Watertown, Massachusetts 02172	15. SECURITY CLASS. (of this report): Unclassified
	15a. DECLASSIFICATION/DOWNGRADING SCHEDULE:

16. DISTRIBUTION STATEMENT (of this Report)

Approved for public release; distribution unlimited.

17. DISTRIBUTION STATEMENT (of the abstract entered in Block 20, if different from Report)

18. SUPPLEMENTARY NOTES

AMMRC TR 81-17

19. KEY WORDS (Continue on reverse side if necessary and identify by block number)

Helicopters	Synthetic fibers
Helicopter rotors	Kevlar
Composite materials	Damage
Braiding	Tolerance

20. ABSTRACT (Continue on reverse side if necessary and identify by block number)

Mechanical tubular braiding has been shown to be a viable blade spar manufacturing process in a program which included preliminary design of an improved main rotor blade for the OH-58 helicopter. The blade incorporates an advanced aerodynamic shape and has as its primary structural member a Kevlar 49®/epoxy spar fabricated by braiding. Achievement of an analytically acceptable blade and spar design meeting critical structural and dynamic requirements was not hindered by braiding process constraints. Mechanical property tests of flat panels and spar sections exhibited excellent

DD FORM 1 JAN 73 1473 EDITION OF 1 NOV 65 IS OBSOLETE

UNCLASSIFIED

SECURITY CLASSIFICATION OF THIS PAGE (When Data Entered)

Block No. 20

correlation with analytical predictions, substantiating the applicability of normal composite laminate analysis methods and the validity of the specific design. Ballistic testing of spar sections demonstrated superior containment of structural damage compared to composite spars produced by more conventional methods. Manufacturing cost estimates predict a price reduction of 1/3 for the braided spar relative to a similar S-glass/epoxy spar for an OH-58 blade of identical external shape fabricated by orthodox, low-cost technology.

PREFACE

Development of tubular braiding as a blade spar manufacturing process, as reported herein, was performed by Kaman Aerospace Corporation under U.S. Army Contract DAAG46-78-C-0070. This project was accomplished as part of the US Army Aviation Research and Development Command Manufacturing Technology program. The primary objective of this program is to develop, on a timely basis, manufacturing processes, techniques, and equipment for use in production of Army materiel. Comments are solicited on the potential utilization of the information contained herein as applied to present and/or future production programs. Such comments should be sent to: US Army Aviation Research and Development Command, ATTN: DRDAV-EGX, 4300 Goodfellow Boulevard, St. Louis, MO 63120.

The Kaman Program Manager was M.L. White and the Army Contracting Officers Technical Representative was initially A. Litman and later P. Dehmer of the Army Materials and Mechanics Research Center (AMMRC).

Kaman was assisted in the development and application of braiding technology by Albany International Research Co. with G. Sharpless as Principal Investigator.

Ballistic testing was performed at the U.S. Army Ballistic Research Laboratory, Aberdeen, Maryland under the direction of C. Green, and at the Applied Technology Laboratory, U.S. Army Research and Technology Laboratories (AVRADCOM), Fort Eustis, Virginia under the direction of C.H. Carper.

The author gratefully acknowledges the contribution to the design, fabrication and testing made by R. Mayerjak, G. Haire, H. Pelletier, E. Nagy, E. Luff and P. Stennett of Kaman and by J. Skelton and E. Kaswell of Albany International Research Laboratories.

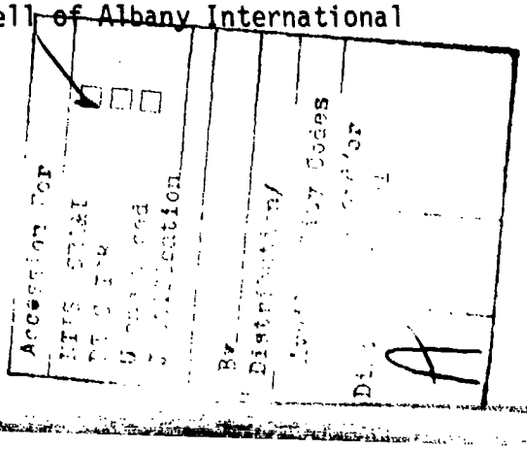

SUMMARY

The U.S. Army and Kaman Aerospace Corporation in their on-going efforts to enhance helicopter blade operational characteristics and reduce manufacturing costs have undertaken the development of mechanical tubular braiding as a composite blade spar manufacturing process. Kaman, the prime contractor, was assisted in the development and application of braiding technology by Albany International Research Company. The program was sponsored by the U.S. Army Aviation Research and Development Command (AVRADCOM) and monitored by the U.S. Army Materials & Mechanics Research Center (AMMRC).

Results of this manufacturing technology program, which included preliminary design of an improved main rotor blade for the OH-58 helicopter, demonstrate the viability of tubular braiding as a blade spar manufacturing process.

The blade design incorporates an advanced aerodynamic shape with double tapered VR-7 airfoil, which has been optimized for the Army's mission requirements without any compromise to accommodate braiding technology. In addition to the leading edge spar, which is fabricated by braiding with Kevlar 49® fiber, the blade structure includes an afterbody of glass fiber/epoxy skin, Nomex® honeycomb core, and a Kevlar®/epoxy trailing edge spline. Blade root attachment is made at bushed holes in the braided spar which mate directly with the existing OH-58 hub and pin.

Detail spar design was accomplished in an integrated program of braiding trials to define attainable fiber orientations coupled with blade design and analysis iterations. Convergence to an analytically acceptable blade and spar design meeting critical structural and dynamic requirements was not hindered by braiding process constraints.

Coupon test panels and spar sections seven feet in length were braided with 7100 denier Kevlar 49® fiber over aluminum alloy mandrels, vacuum impregnated with liquid resin, autoclave cured, and tested. Reproducibility of fiber angles was well within conventional composite tolerances. Material property tests and spar section tests exhibited excellent correlation with analytical predictions, substantiating the applicability of normal composite laminate analysis methods to braided composites, and the validity of the specific design.

Ballistic testing of spar sections against the .30 caliber fragment simulator projectile and the .50 caliber APM2 projectile demonstrated superior containment of damage for the interwoven braided structure compared to a similar spar of wound S glass. It should also be noted that testing by Kaman on earlier programs has shown that helical filament winding, which produces a limited degree of interweaving, results in improved ballistic tolerance versus tape layup.

Manufacturing cost estimates comparing the braided Kevlar®/epoxy spar with a similar filament wound S glass/epoxy spar for an OH-58 blade of identical external shape showed a 33% cost reduction for the braided design in quantities of 500.

TABLE OF CONTENTS

LIST OF ILLUSTRATIONS

LIST OF ILLUSTRATIONS (Cont'd)

LIST OF TABLES

INTRODUCTION

The U.S. Army and Kaman Aerospace Corporation in their on-going efforts to enhance helicopter blade performance and reduce manufacturing costs have undertaken the development of mechanical tubular braiding as a composite blade spar manufacturing process. Fiber/resin composite construction has engendered a new generation of helicopter blades of vastly improved performance, reliability and maintainability. The first process employed for blade spar manufacturing was layup of unidirectional prepreg (references 1 and 2). More recently, filament winding has been introduced as a lower cost, automated production process (references 3, 4 and 5). Mechanical braiding is of interest for blade spar manufacturing primarily because, while it has a considerable similarity to filament winding, it has a demonstrated capability of automated fiber lay-down at substantially higher rates than are achieved with conventional winding. Further, braiding can efficiently produce layers of nearly spanwise fibers as well as for oblique helical layers in a single machine whereas these operations are more effectively performed in separate machines and operations when filament winding is employed.

Braiding is an old, established textile process for producing a woven tubular fabric using a machine of the type shown in Figure 1. In operation, the braider carriers holding spools, or cops, of fiber are driven through intersecting serpentine slots around the large, stationary outer ring. Half of the carriers revolve in one direction and half in the other, passing over and under each other as they orbit the center of the ring, weaving the fibers into a tubular fabric. The over-two, under-two pattern produced, which is similar to a twill weave, is illustrated in Figure 2.

For more than a century, tubular braiding has been employed in fabricating prosaic textile products, such as shoelaces, rope, fabric hose and braided overlays on cable assemblies. In more recent times, the process has been adapted to composite fabrication (references 6 and 7), predominantly in light duty for nonstructural applications such as aircraft ducting.

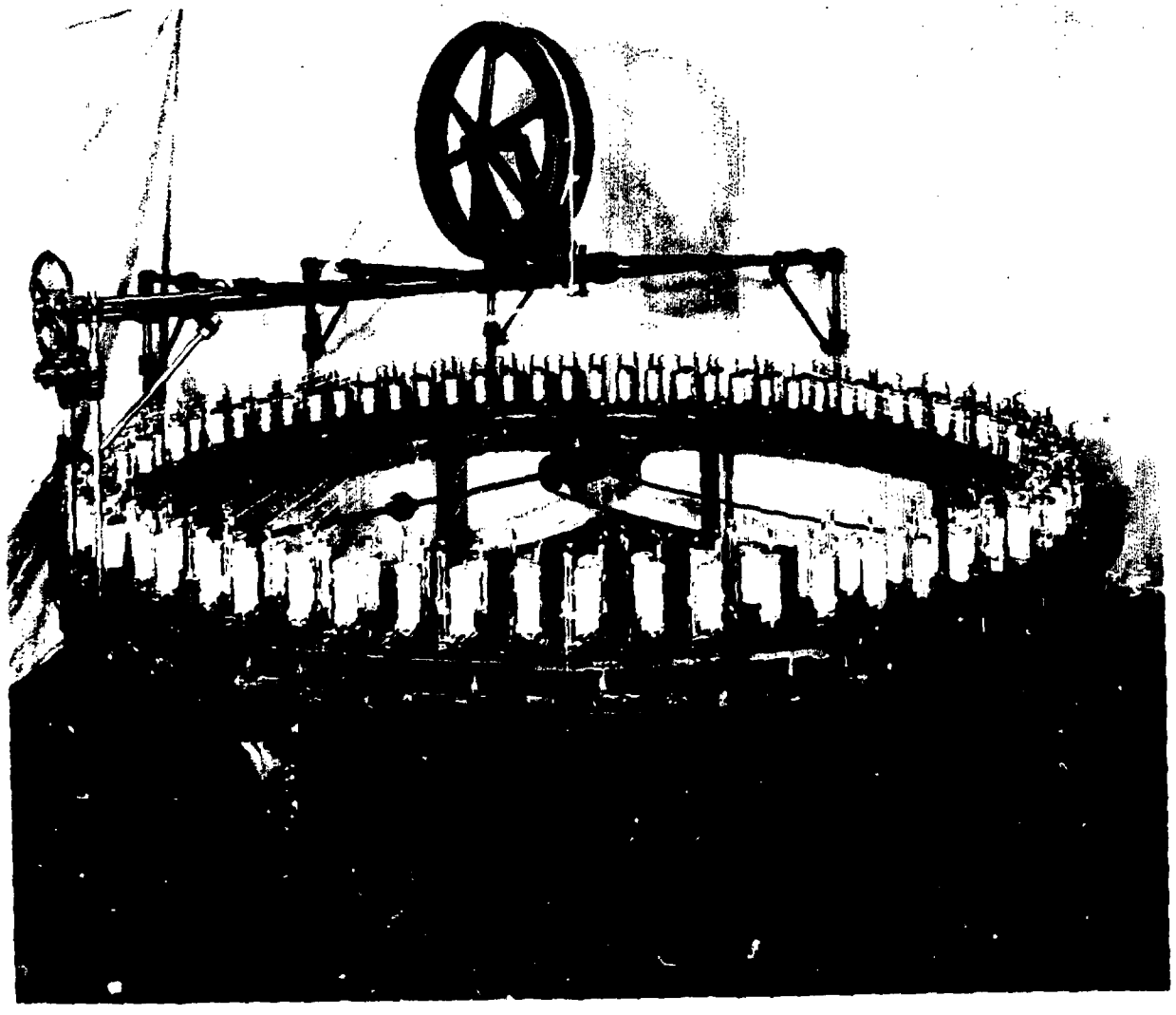

Figure 1. Large braiding machine manufactured by New England Butt Company.

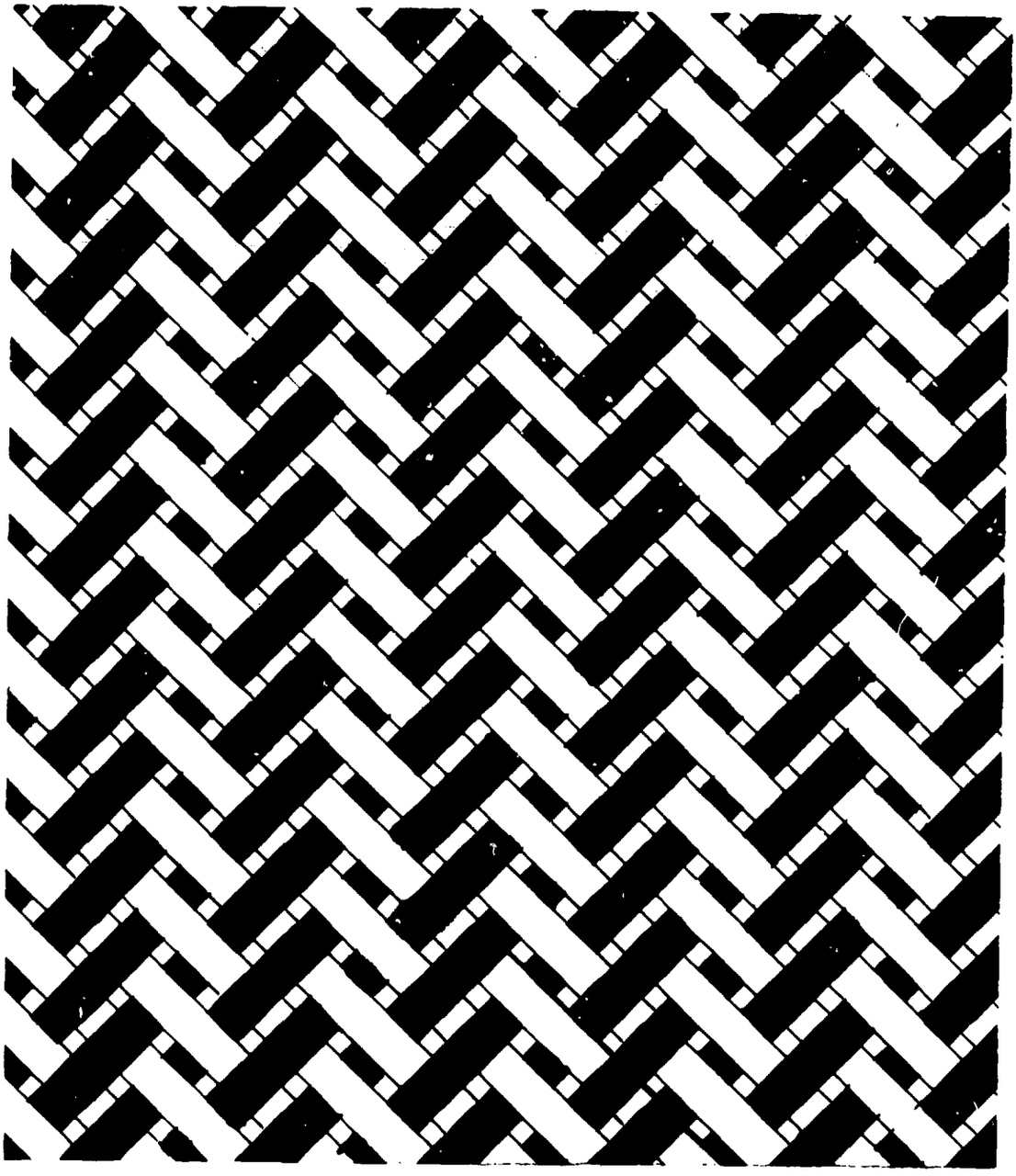

Figure 2. Illustration of braid weave.

Figure 3 shows a conventional braiding machine which has been adapted for the fabrication of composite structure having controlled fiber orientation. This modification consists simply of the addition of a mechanism for translating a nonrotating mandrel, upon which the braided fabric is deposited, through the braider at a controlled pitch (i.e., distance of mandrel travel per revolution of the braider carriers). The control of fiber orientation angle afforded by this means of governing the relative motion of the evenly wrapped fibers and the mandrel is geometrically analagous to the filament winding process. In conventional filament winding, a carriage translating at controlled pitch lays out a fiber band onto a rotating mandrel. In a variant of conventional winding, called ring winding, the payout head is mounted on a ring which rotates around the mandrel.

In contrast to the filament winding processes as normally employed, tubular braiding deposits a much higher number and volume of filaments simultaneously. Increases in fiber laydown rates of approximately 20 to 30 times can be readily achieved with available equipment. This factor, together with the effect of the interlocked braided layers in preventing fiber slippage, make the fabrication of braided layers with nearly spanwise orientation practical; a significant manufacturing economy.

Additionally, the high level of interweaving inherent in braided composite is expected to impart yet a greater degree of ballistic tolerance than that achieved with filament winding. Previous work (reference 4) has shown that the limited interweaving produced by filament winding enhances ballistic tolerance in comparison to structures laid up from unidirectional prepreg layers.

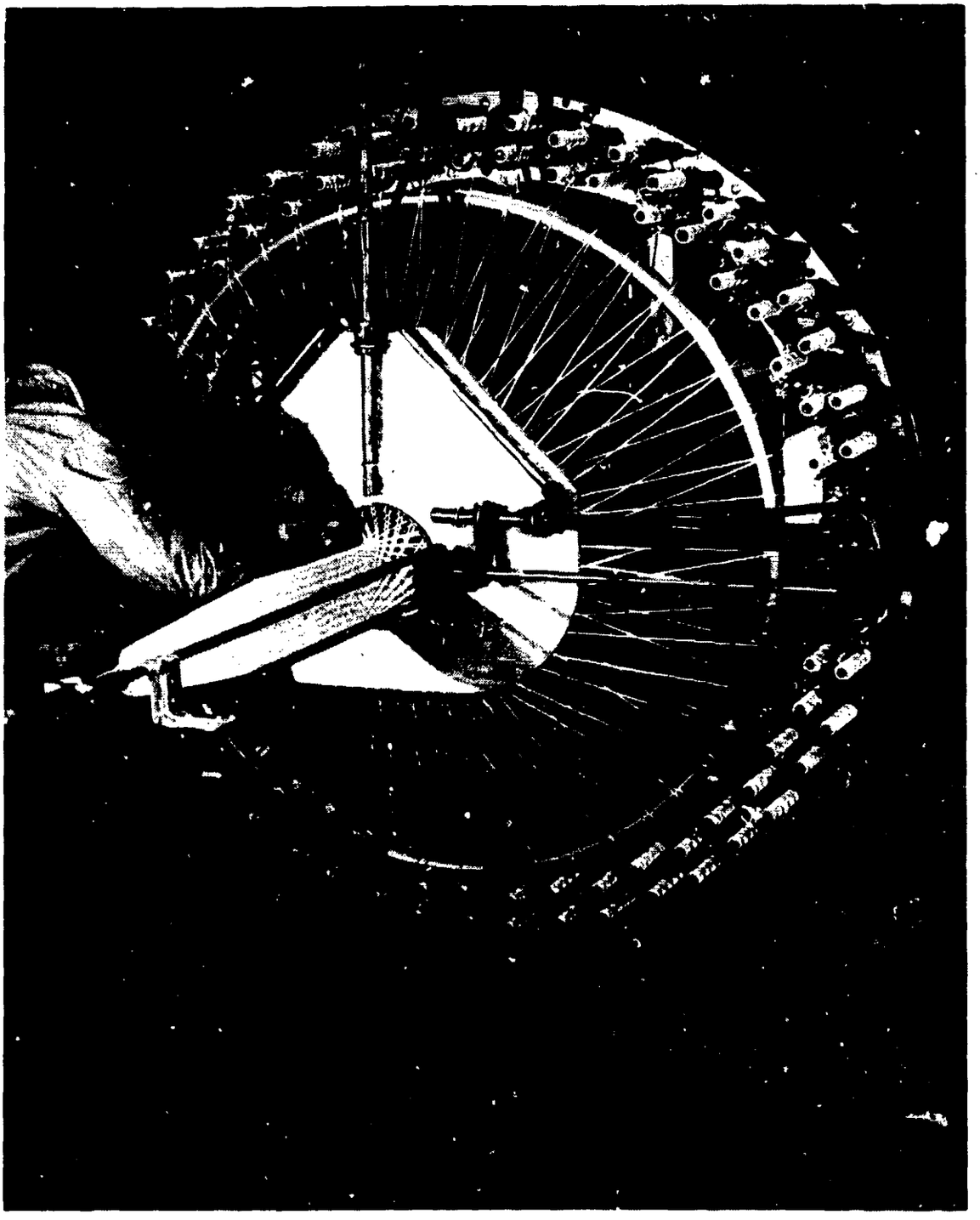

Figure 3. Composite braiding.

DESIGN AND PROCESS DEVELOPMENT

Technical Approach

An OH-58 blade shape having an advanced aerodynamic geometry optimized for the Army's mission requirements in an earlier Kaman study (reference 8) was used as a basis for the braided spar blade design. Cost studies and ballistic testing performed on the S Glass/epoxy wound spar design developed in that program afforded an opportunity for direct, meaningful comparison of relative cost and ballistic tolerance between filament wound and braided spars.

As in the AH-1 composite blade development program (references 3 and 4) and in the OH-58 blade design study (reference 8), matching of the natural frequencies of the existing metal blade was chosen as the least risk method of assuring dynamic compatibility with the OH-58 helicopter.

With the desired external shape, and the mass and stiffness distribution constraints thus defined, an integrated program of braiding studies to define fiber braiding characteristics and attainable orientations coupled with blade design and analysis iterations was initiated.

Structural analysis followed, generally, the procedures described in reference 8. Laminate strengths and stiffnesses were calculated using Kaman computer code CMAB (Composite Materials Analysis version B) which considers the properties of each lamina in deriving the properties of the overall laminate. In analyzing the braided composite, each braided layer was replaced by two laminae of half layer thickness, one representing the positive, and one the negative fiber angles of the bidirectional fabric. The validity of this procedure was subsequently verified by mechanical property testing reported below.

Blade/Spar Configuration and Fabrication

Figure 4 illustrates the OH-58 braided spar composite blade design and tabulates its basic dimensional characteristics and those of the standard OH-58 blade. The KA 757 blade incorporates an advanced aerodynamic shape with double tapered planform, VR-7 airfoil, and 12 degree twist from center of rotation to tip which has been optimized for the Army's mission requirements without any compromise to accommodate braiding technology. In addition to the leading edge spar, which is fabricated by braiding with Kevlar 49® fiber, the blade structure includes an afterbody of glass fiber/ epoxy skin, Nomex® honeycomb core, and a Kevlar® /epoxy trailing edge spline. Blade root attachment is made at bushed holes in the braided spar which mate directly with the existing OH-58 hub and pin. Cross sections of the KA757 blade at stations 36.5 and 179.916 are shown in Figures 5 and 6.

A substantial bundle of molded unidirectional E-glass/epoxy is overbraided into the spar leading edge and becomes an integral part of the structure. This more dense fiberglass composite member at the leading edge provides ballast needed to achieve the required 1/4 chord location of the center of gravity and also improves tolerance to such events as tree strikes and ballistic impact. In addition, an elastomer coated metal weight is overbraided and bonded into the spar tip to achieve dynamic tuning and the polar moment of inertia required for autoration characteristics. Both of these features are employed in the production of the AH-1 composite improved main rotor blade (references 3 and 4).

Appendix A is a structural analysis report demonstrating adequate strength and appropriate stiffnesses for the KA 757 blade. Detailed analysis of the blade between stations 70 and 179.9 was performed. Analysis of the root and tip regions and final dynamic tuning were beyond the scope of the contract, but preliminary studies and the similarity of the KA 757 blade spar to the spar design of reference 8 leave no doubt that a satisfactory overall design can be achieved.

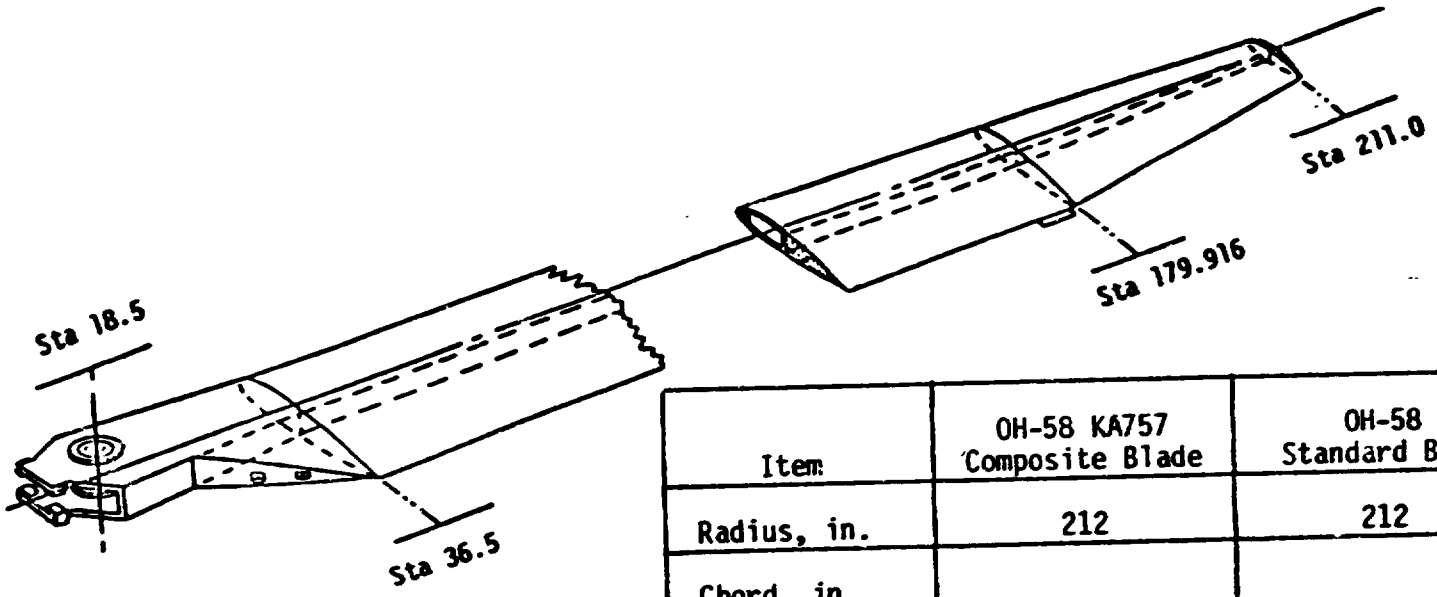

Item	OH-58 KA757 Composite Blade	OH-58 Standard Blade
Radius, in.	212	212
Chord, in. Sta 36.5 Sta 179.916 Sta 211	 15 12.5 6.14	 13 13 13
Weight, lb	<95	95

Figure 4. Comparative information - OH-58 blade.

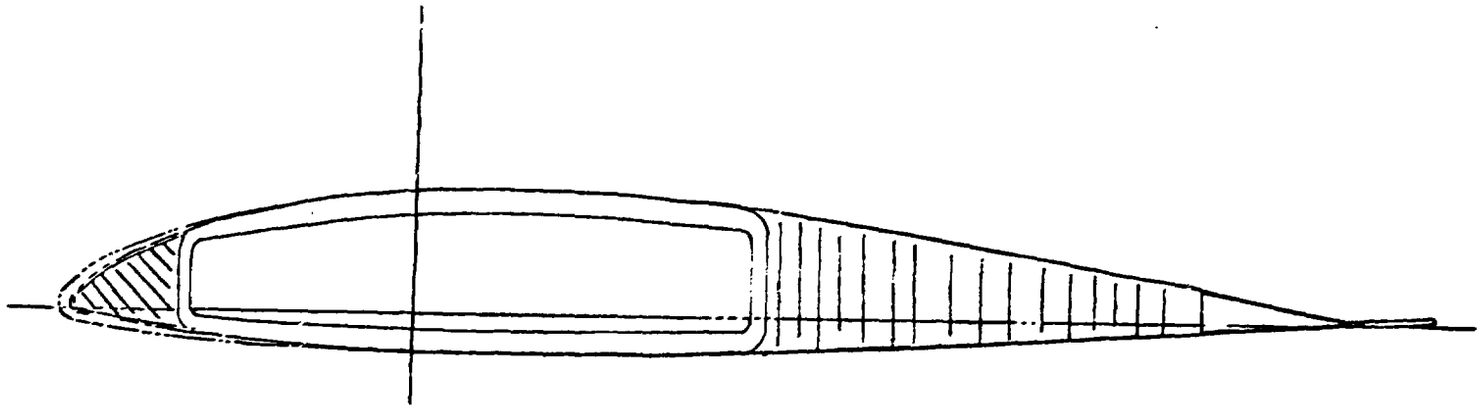

Figure 5. KA757 Blade - Sta. 36.5.

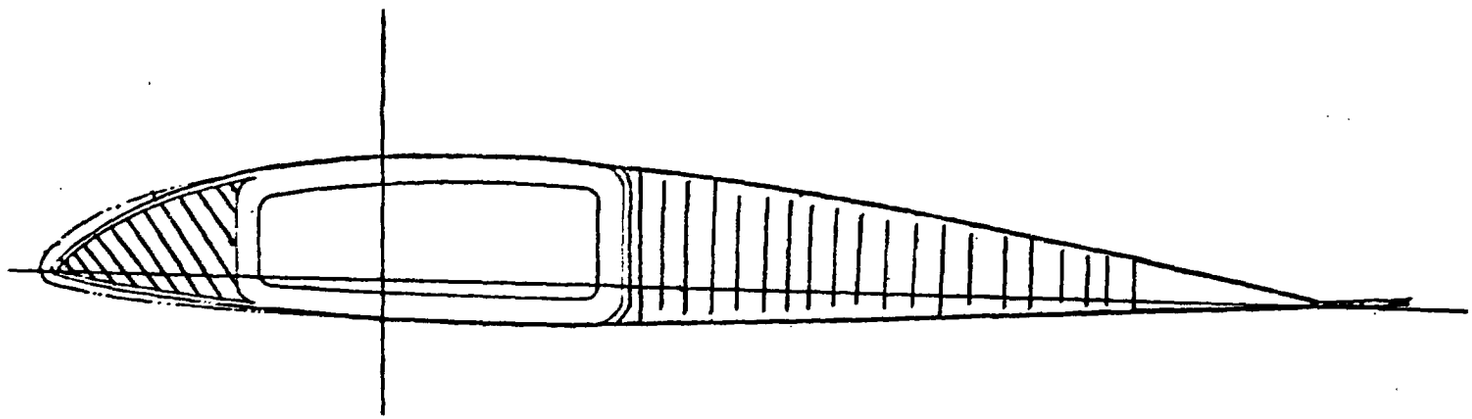

Figure 6. KA757 Blade - Sta. 179.9.

Spar braiding is carried out with 7100 denier roving. Twelve braided layers, four low angle layers (designated α) and eight high angle layers (designated β), run from root to tip. The layer sequence is $\beta, \beta, \alpha, \alpha, \beta, \beta, \beta, \beta, \alpha, \alpha, \beta, \beta$. These fiber angles are measured from the spar longitudinal axis. The low angle, nearly spanwise, layers provide longitudinal strength and stiffness while the higher angle layers satisfy torsional and chordwise property requirements.

For simplicity of manufacture, each braided layer is designed to be applied at a constant pitch (i.e., mandrel advance per revolution of the braider carriers) allowing the fiber orientation angle to decrease and the layer thickness to increase as circumference decreases along the tapered spar. Braid angle and layer thicknesses versus blade station are given in Appendix A.

The outer two braid layers envelope the molded glass/epoxy leading edge member. Additional fabric laminae are interleaved between the braid layers inboard of station 60 as required for local stiffening and to achieve required bearing and section strength at the blade attachment holes. The addition of interleaved doublers, which is commonly employed with filament wound spars, is even simpler when braiding on a nonrotating mandrel.

Blade manufacturing initiates with braiding of dry roving on an aluminum alloy mandrel having the tip weight attached at the outboard end. This weight is, in effect, a part of the mandrel which becomes a permanent part of the spar. The dry braided spar assembly (with inserted doublers and leading edge filler) is then vacuum impregnated with a liquid epoxy resin in a matched tool to provide accurate control of resin content. Spar and blade afterbody details are cocured in a matched steel mold. Mandrel withdrawal is performed before the addition of the bushings, closures and trim weights to complete the blade. The use of hard internal mandrels and external molds assures precise contour fidelity and weight control, and is the same basic tooling concept proven in the AH-1 composite blade production program (references 3 and 4).

An engineering specification for fabrication of spars by tubular braiding is presented in Appendix B.

Development Testing

Fabrication trials, flat laminate mechanical property tests, spar section structural and ballistic tests, and nondestructive inspection evaluations were conducted. In the course of the program coupon test panels and two seven foot spar sections were fabricated.

Preliminary substantiation of analytically predicted properties, impregnation development, and evaluation of braiding orientation reproducibility was performed on flat panels fabricated on aluminum plate mandrels. Three foot long mandrels having a cross section 3/8 inch by six inches were overbraided with six layers in the sequence ±46°/±46°/±15°/±15°/±46°/±46°. This mandrel circumference is equal to that of the spar inner surface at blade station 80, and the layer sequence represents one-half the spar wall at that station.

Measured fiber angles of each layer of each of five separate panels braided were uniformly of the orientation stated above within the accuracy of protractor measurement (≈ 1°).

Vacuum impregnation was performed with the liquid epoxy/aromatic amine resin system of Appendix B. The part was enclosed in a nylon film bag of the type normally used for autoclave curing. This bag was sealed to the mandrel ends and the resin introduced through a perforated tube extending through the bag seal. Figures 7 and 8 illustrate this impregnation process being performed on one of the spar sections produced subsequently. Impregnation was followed by rebagging and autoclave curing.

One of the flat panel specimens was selected for mechanical property testing and examined for laminate quality. Microexamination of polished transverse and longitudinal sections through the thickness of laminate near the center of each three foot by six inch face of specimen revealed sound, low void laminate quality. Gravimetric analysis combined with nitric acid digestion per ASTM D3171-76 at locations adjacent to the micro samples revealed resin contents of 41.9% and 46.0% by weight and void contents of 2.75% and 2.46%, respectively.

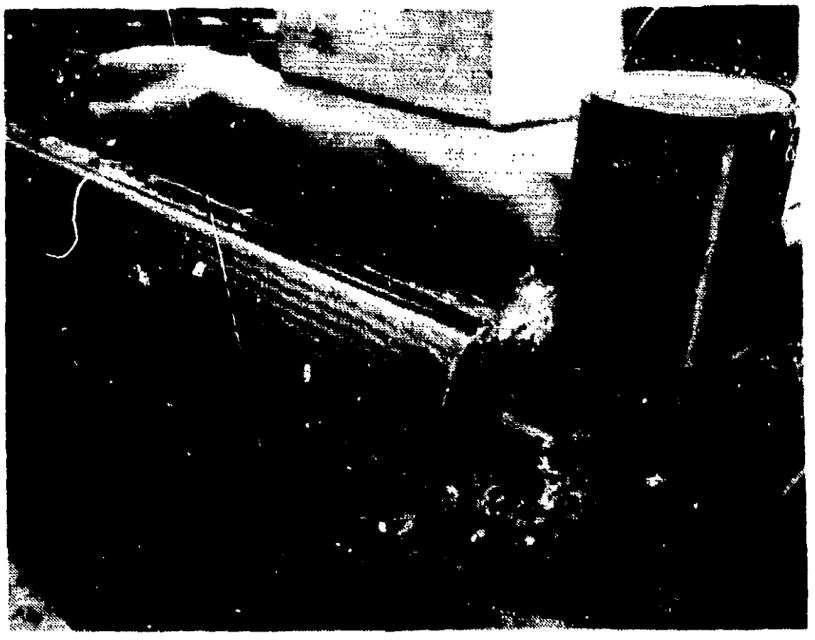

Figure 7. Vacuum impregnation - resin feed end.

Figure 8. Vacuum impregnation - pump end.

In-plane shear properties, and longitudinal and transverse tensile and flexural properties of the test laminate were determined at room temperature on specimens which were conditioned indoors for two to six weeks between laminating and testing. Tensile testing was performed per ASTM D 3039-76, in-plane shear testing by the rail shear method of reference 9, and flexural testing per ASTM D 790-71, Method 1, Procedure A. Test results are reported in Table 1. The tensile and shear properties are based on the .090 inch nominal panel thickness (55 volume percent fiber) to agree with the structural analysis.

For comparison, Table 1 also includes the analytically predicted properties of the spar wall at station 80 as reported in Appendix A, Table A-2 and Figures A-7 and A-8. The test laminate represents one-half the spar wall at station 80. Elastic moduli are in good agreement with the analytical predictions while ultimate strengths exhibit large margins above predicted allowable stresses. The calculated strengths are conservative estimates corresponding to the first failure of an individual ply, and are typically lower than observed ultimate failure stresses.

Two seven foot spar sections, one containing the fiberglass nose piece and one without, were fabricated on an aluminum alloy mandrel having the contour of the spar internal surface at station 80 and a constant taper of .005" per foot. Impregnation and autoclave curing were performed as on the panel specimens. Edgewise bending, flapwise bending and torsional static tests were performed on these sections. Measured stiffnesses correlated well with analytical predictions, and design limit loads were sustained without damage or deformation. In addition, moments equivalent to 110 percent of design ultimate load in flatwise bending were applied to one section and maintained for ten minutes without failure. Figures 9 and 10 illustrate the flatwise bending and torsional tests, and load-deflection results of one torsion test and one flatwise bending test are plotted in Figures 11 and 12.

TABLE 1. MECHANICAL PROPERTIES
KEVLAR/EPOXY BRAIDED LAMINATE

Property			Test Values	Predicted Values
Longitudinal Tensile Strength	Fx^{tu}	(psi)	50,391	38,980
Individual Values: 53,865 - 54,495 - 46,749 - 45,685 - 50,963				
Standard Deviation	σ	(psi)	3544	
Longitudinal Tensile Modulus	Ex^{t}	(psi)	3.1×10^6	3.0×10^6
Longitudinal Elongation at Max Stress	ϵx^{tu}	(%)	1.85	--
Poisson's Ratio	μxy		0.95	
Transverse Tensile Strength	Fy^{tu}	(psi)	13,997	--
Individual Values: 13,603 - 12,566 - 13,705 - 15,083 - 15,030				
Standard Deviation	σ	(psi)	952	
Transverse Tensile Modulus	Ey^{t}	(psi)	1.6×10^6	1.7×10^6
In-Plane Shear Strength	Fxy^{su}	(psi)	28,699	13,870
Individual Values: 26,586 - 26,041 - 29,696 - 31,603 - 29,568				
Standard Deviation	σ	(psi)	2084	
In-Plane Shear Modulus	Gxy	(psi)	2.0×10^6	2.1×10^6
Longitudinal Flexural Strength		(psi)	51,534	--
Individual Values: 58,664 - 49,646 - 48,820 48,860 - 51,681				
Standard Deviation	σ	(psi)	3713	
Transverse Flexural Strength		(psi)	37,259	--
Individual Values: 38,136 - 37,384 - 37,984 37,501 - 35,290				
Standard Deviation	σ	(psi)	1024	

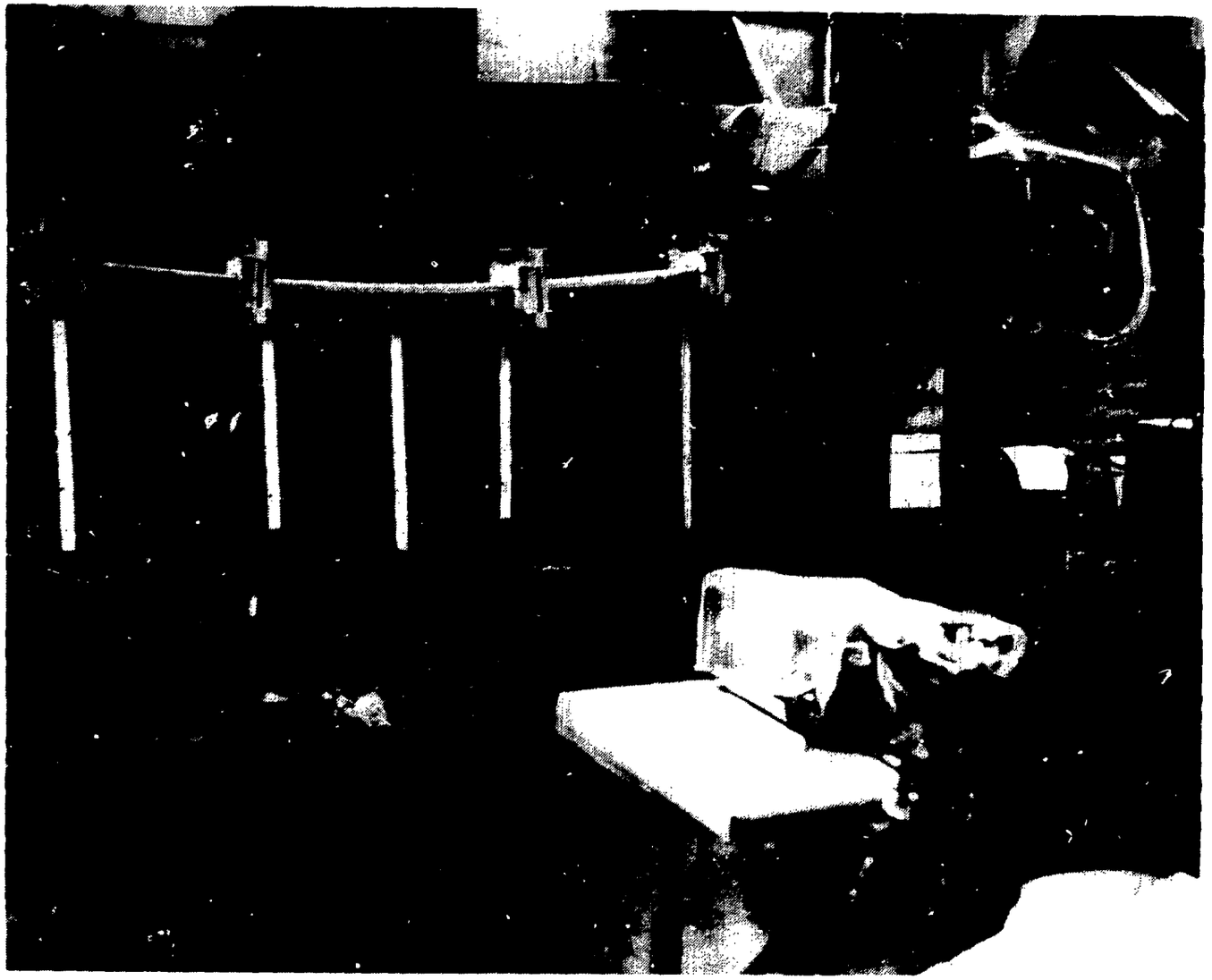

Figure 9. Flatwise bending test - 110% design ultimate load.

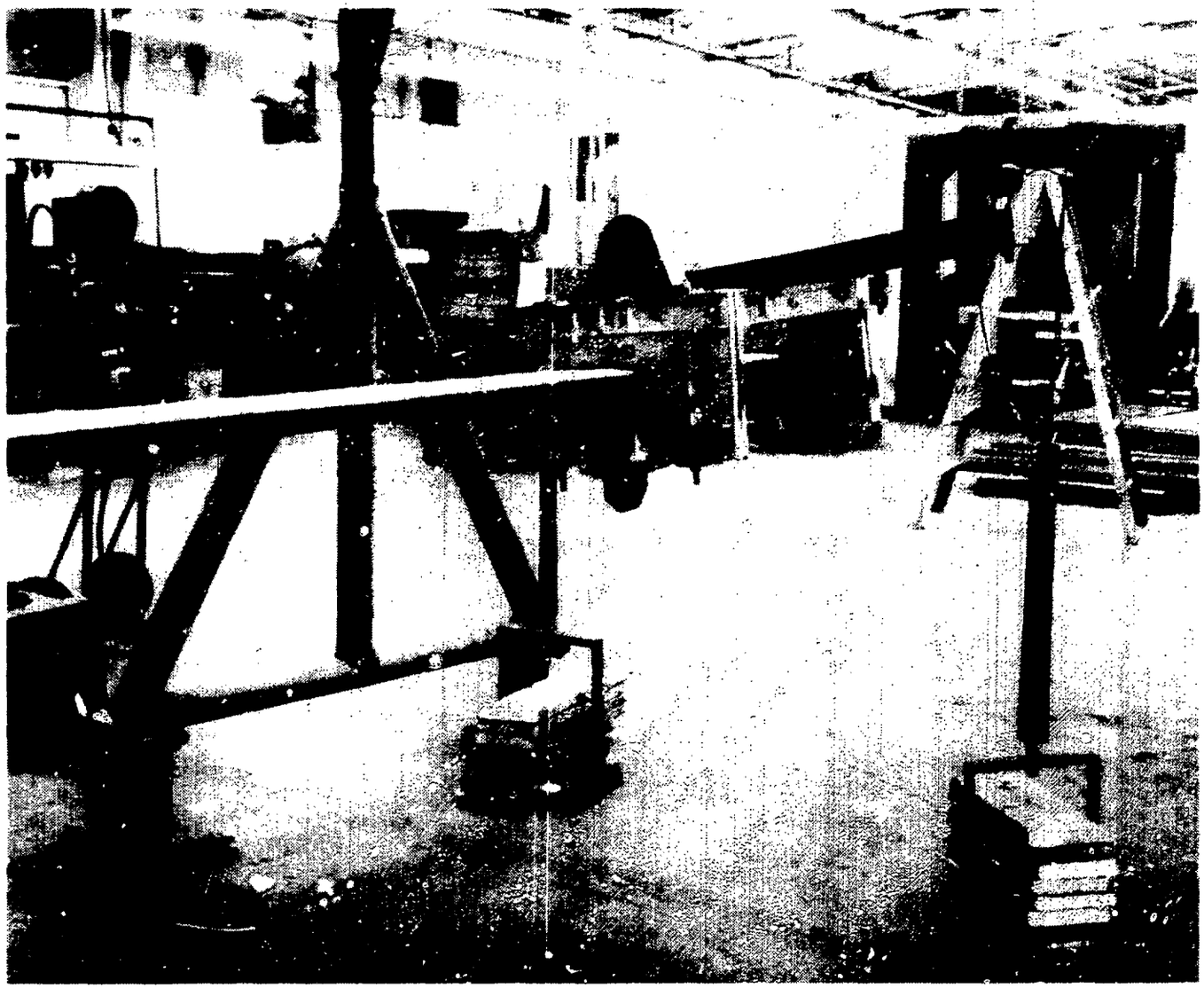

Figure 10. Torsion test - 100% design limit load.

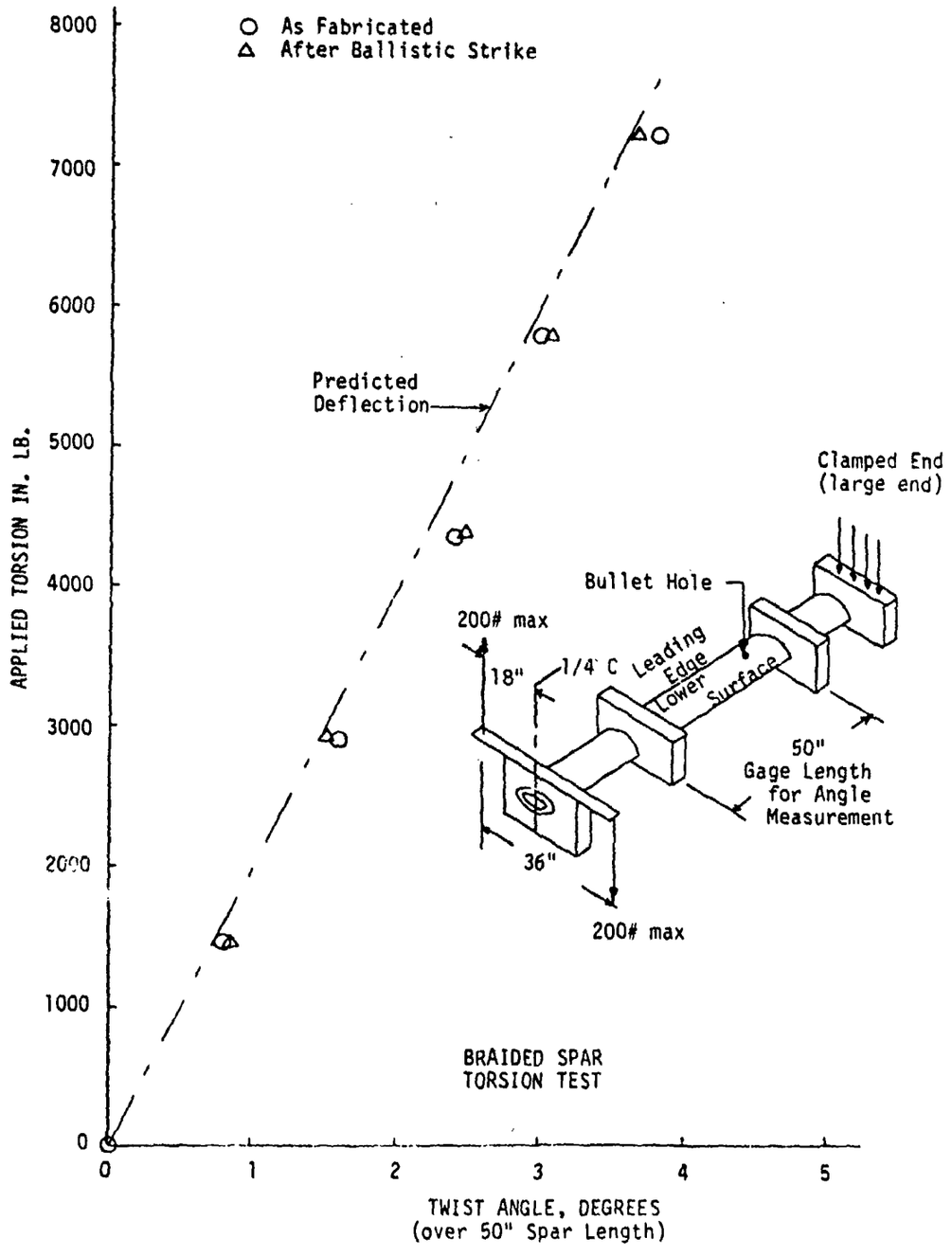

Figure 11. Braided spar torsion test.

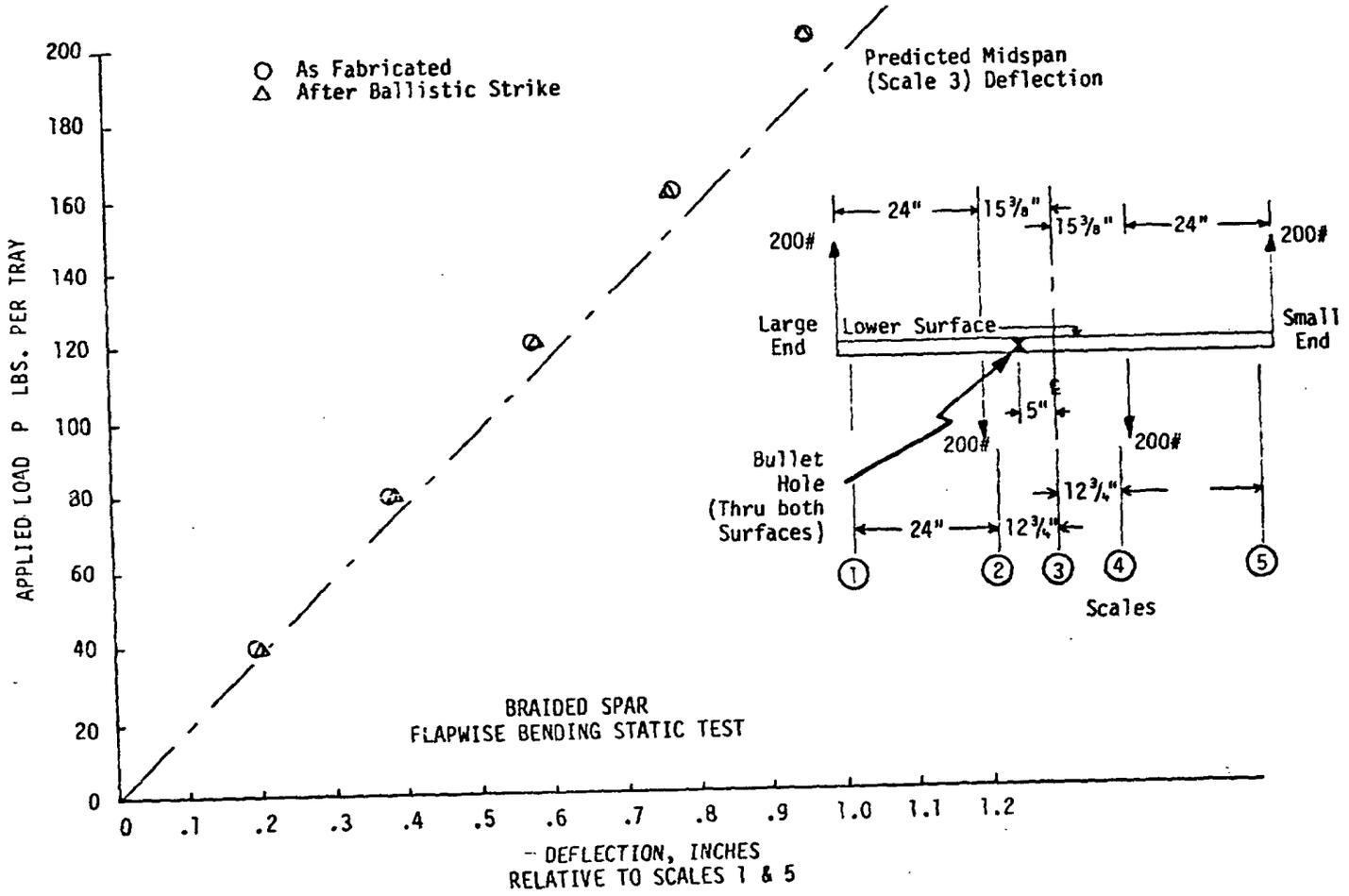

Figure 12. Braided spar flapwise bending test.

One spar section was impacted with a .30 caliber fragment simulator projectile which penetrated through both walls of the spar. Figures 13 and 14 show the entrance and exit surfaces, respectively. Visually apparent damage does not extend much beyond the actual projectile hole. Ultrasonic inspection, described below, revealed roughly circular areas of delamination extending up to one inch beyond the holes. Static retesting of the spar section in flatwise bending and torsion to limit loads showed no detectable changes in elastic properties, and resulted in no apparent extension of the damage.

A second spar section was struck with a fully-tumbled, .50 caliber armor piercing projectile in a manner duplicating as closely as possible the similar test reported in reference 8. Figure 15, 16 and 17 show the projectile impact and exist surfaces of that spar, and reveal damage extending only slightly beyond the actual puncture. In comparison the conventionally fabricated fiberglass spar of reference 8 (see, for example, the equivalent photograph from that report) exhibited extensive fracture and brooming of spanwise fibers, and delaminations extending several inches beyond the point of impact.

Both ballistic tests indicate that the OH-58 braided spar has a high degree of survivability to .03 caliber and .50 caliber projectiles which is enhanced by the effect of the tightly woven structure of the braided composite in containing the extent of damage. This result is not surprising inasmuch as previous Kaman testing (reference 4) has shown that helical filament winding, which produces a limited degree of interweaving, results in improved ballistic tolerance versus tape layup. The fact that the nearly spanwise fibers are also braided is particularly significant. Such low angle layers cannot be practically produced by filament winding, and separately wound, unidirectional, spanwise layers are normally employed between the helical layers of filament wound spars.

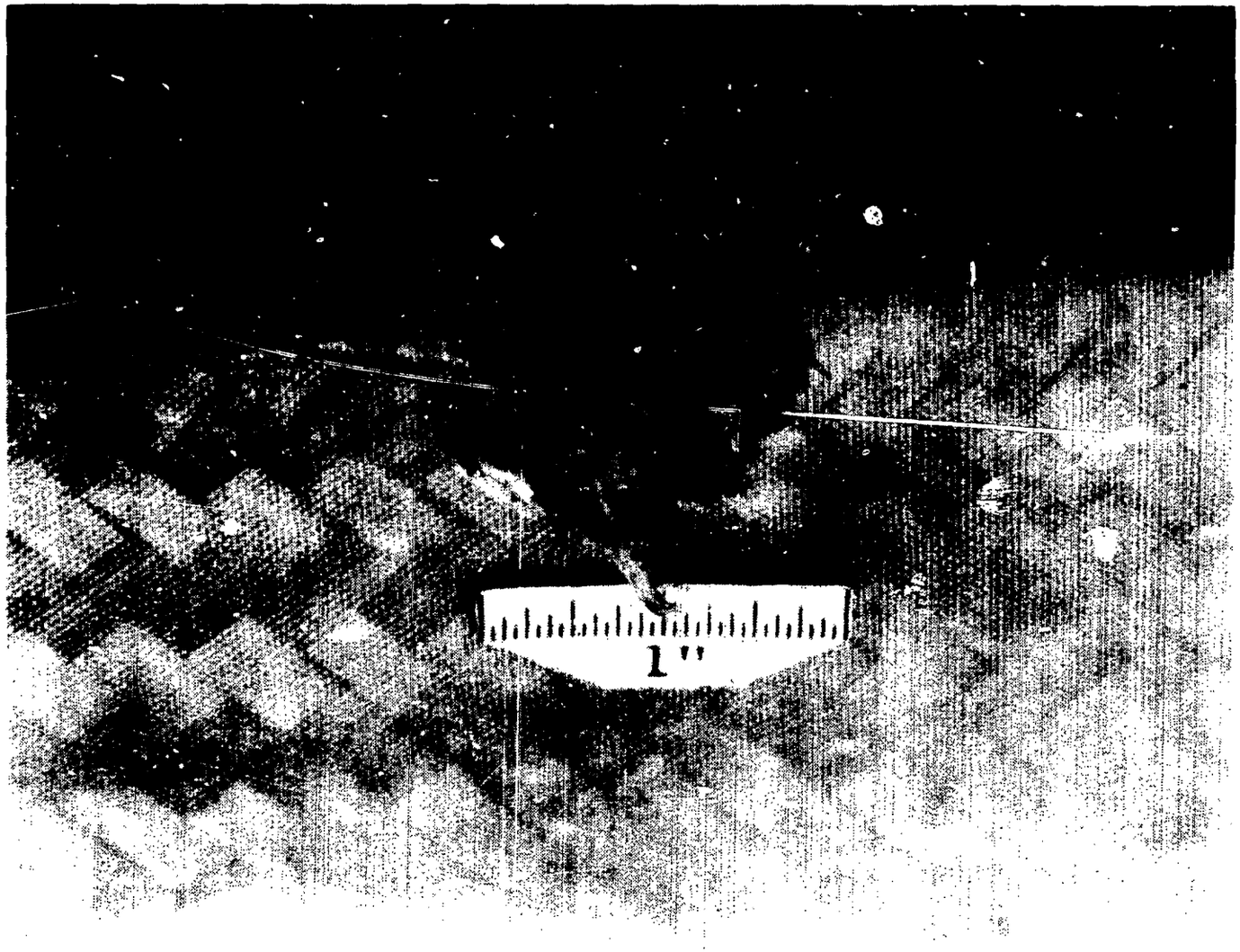

Figure 13. Braided spar entry area of .30 caliber fragment simulator projectile on bottom surface near leading edge.

Figure 14. Braided spar exit of .30 caliber fragment simulator projectile on top surface.

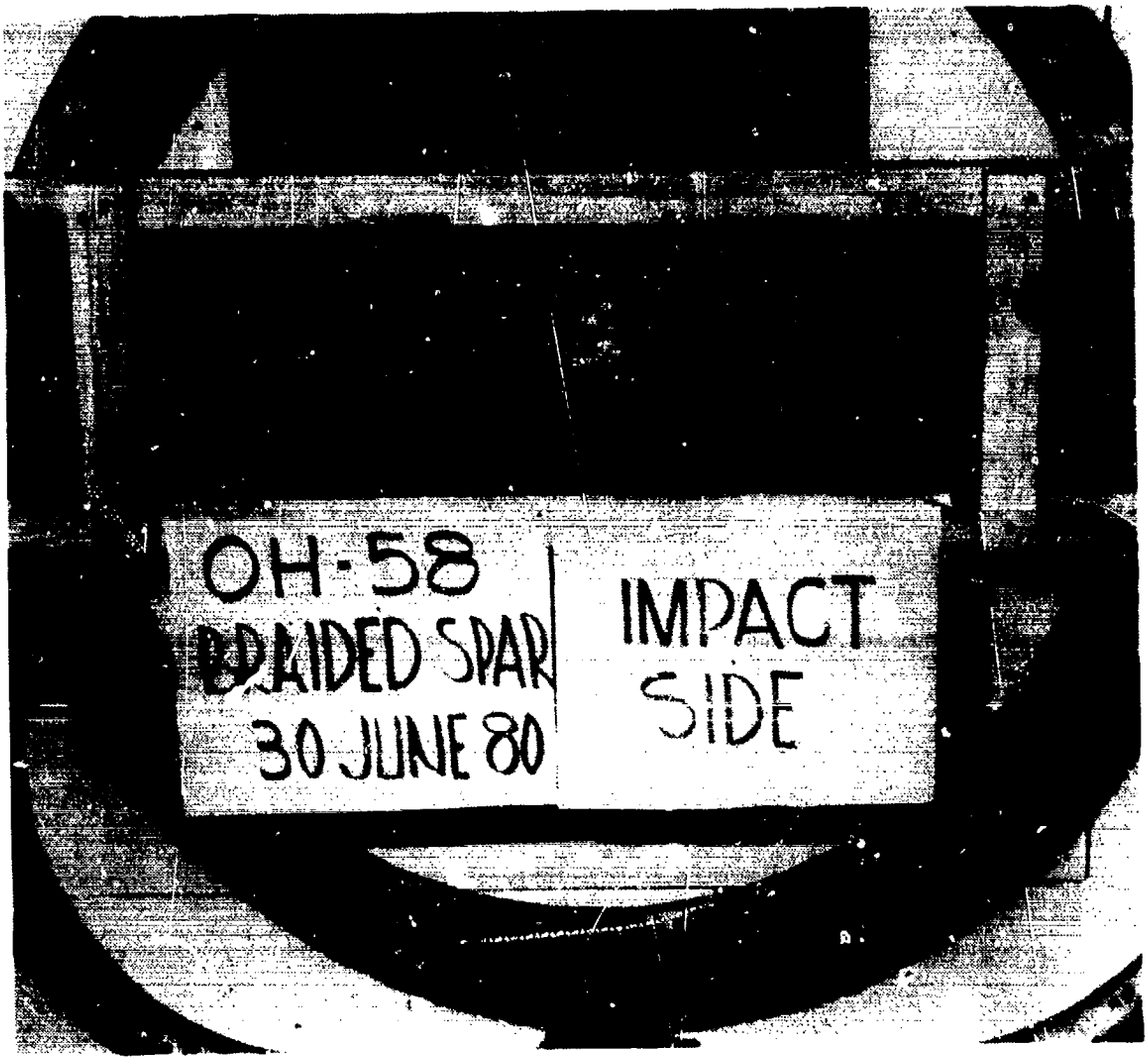

Figure 15. Impact side - .50 caliber tumbled strike.

Figure 16. Exit side - .50 caliber tumbled strike.

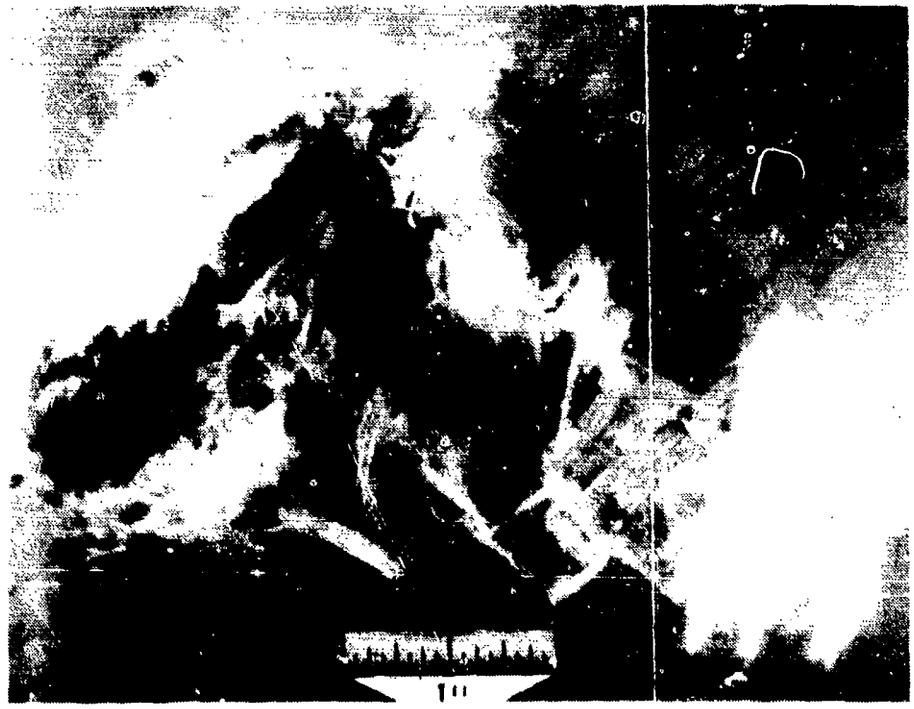

Figure 17. Tumbled .50 caliber projectile exit side.

Inspectability is an important characteristic of any composite blade design. Therefore, development of a C-scan, through transmission ultrasonic inspection technique was undertaken to assure that this method, which is commonly used for inspecting other composite spars, is adequately sensitive to discontinuities in braided composite spars. Figure 18 is a C-scan chart record of a spar section illustrating a capability for resolving the smallest (1/4 in. x 1/2 in.) simulated defect evaluated. This chart also includes an area struck with a .30 caliber fragment simulator projectile and shows both the open holes, which permit sound transmission, and the small area of delamination surrounding the holes.

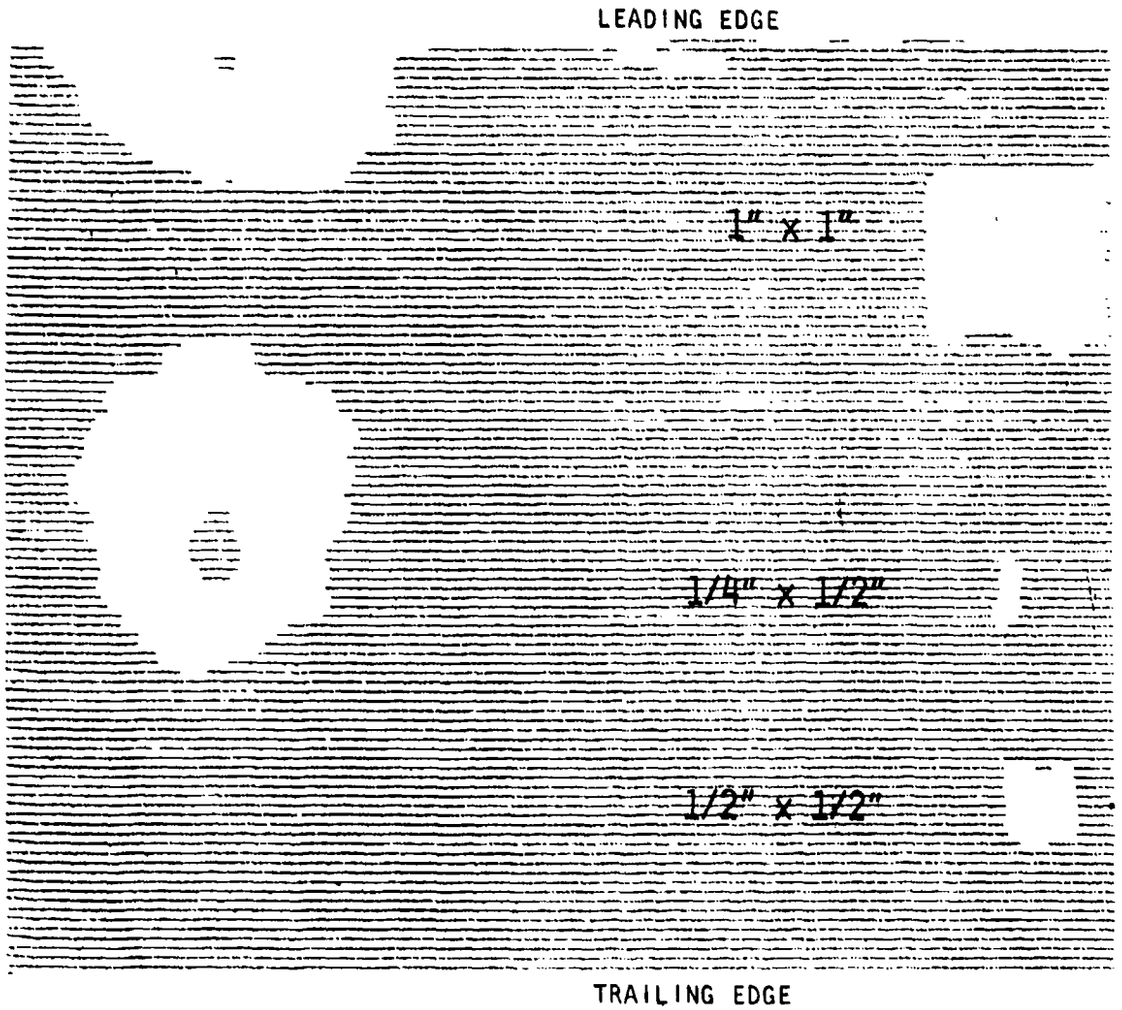

Figure 18. Ultrasonic C-scan record showing simulated defects and ballistic strike area.

MANUFACTURING COST ANALYSIS

Detailed estimates of average spar prices in production runs of 200 and 500 units were prepared for the braided Kevlar® spar, the similar wet filament wound fiberglass spar of reference 8, and the metal spar of the present OH-58 blade using typical Aerospace Industry cost estimating procedures. Material requirements, including waste factors, and labor hours for the braided spar were based on data collected during spar section fabrication. Kaman experience in fabricating both filament wound and metal spar blades provided similar basic information for those estimates. A ninety percent experience curve was assumed for all manufacturing operations. Representative Aerospace Industry material prices, and labor and burden rates for 1980 were employed in calculating costs.

Table 2 summarizes these estimates, which predict a 1/3 price reduction for the braided Kevlar spar in comparison to the filament wound glass version. Since the remainder of the structure and associated manufacturing processes for both composite blades are nearly identical, equivalent dollar savings would be projected for the complete braided spar blade. Further, in reference 8, wet filament winding was chosen as the lowest-cost, established composite spar manufacturing process. Therefore, even greater savings would be expected versus other methods, such as tape layup.

A more detailed breakdown of estimated direct labor manhours for producing the braided and filament wound OH-58 composite spars is given in Table 3. The machine setup time for braiding includes the labor required for winding of roving onto the braider cops, and installation of the cops into the braiding machine. Winding of the braider cops from standard, ten-pound spools of roving using a conventional, six-stand bobbin winder is assumed. One loading of the 96 carrier braider is required to produce one spar.

TABLE 2. SUMMARY OF ESTIMATED PRODUCTION COSTS

OH-58 BRAIDED KEVLAR, FILAMENT WOUND S-GLASS ALUMINUM SPARS

200 AND 500 SPARS - 1980 DOLLARS

ITEM	BRAIDED SPAR		FILAMENT WOUND SPAR		METAL SPAR	
	200	500	200	500	200	500
Materials (Burdened)	310	310	171	171	1035	1035
Labor Burdened	645	561	1285	1120	672	584
Other Direct Costs	25	21	50	43	28	25
Unit Price (with 10% Profit)	1078	981	1657	1467	1909	1808
TOTAL PRICE (200 or 500 UNITS)	$215,600	$490,500	$331,400	$733,500	$381,800	$904,000

TABLE 3. DIRECT LABOR MANHOURS/SPAR
BRAIDED KEVLAR VS. FILAMENT WOUND S-GLASS
AVERAGE OF 200 SPARS

Operation Category	Direct Labor Manhours	
	Braided Spar	Filament Wound Spar
Machine Setup	3.2	2.8
Spar Braiding or Winding	5.9	25.2
Impregnation & Staging (Resin Transfer Molding)	3.3	N.A.
Bleed, Debulk & Stage	N.A.	2.9
Fabrication of Molded Leading Edge Filler	6.2	6.2
Miscellaneous Labor	4.4	8.7
Total Direct Labor	23.0	45.8

Both composite spars are estimated to be less expensive than the standard metal spar. However, the afterbody details of the constant section metal blade (basically, stamped aluminum alloy skins, aluminum honeycomb core and an aluminum alloy wedge extrusion) are not directly comparable to the equivalent components of the composite blades. Therefore, the spar cost figures do not reflect a finished blade cost comparison between the metal and composite blades.

CONCLUSIONS

- Mechanical braiding is a viable manufacturing technology for helicopter main rotor blade spars. Application of the braiding process did not inhibit design of an advanced geometry blade for the OH-58 helicopter.

- Conventional laminate analytical methods accurately predict the performance of composites produced by braiding.

- Braiding can produce major reductions in composite spar manufacturing costs.

- The interwoven structure of a braided spar laminate contains the extent of ballistic damage to a greater degree than does the more limited interweaving of a filament wound structure. Both are ballistically more tolerant than laminates of angleplied unidirectional prepreg.

REFERENCES

1. Wells, E., "Summary of Test Data, Glass Fiber Rotor Blades," Report T-379, Kaman Aircraft Corporation, Bloomfield, Conn., August 1962.

2. Field, D.M., Finney, R.H. & Stratton, W.K., "Achieving Fail Safe Design in Rotors," Preprint No. 673, 28th Annual National Forum of the American Helicopter Society, May 1972.

3. Maloney, P.F., Dite, L.G. and Powell, R.D., "The Army's Improved Main Rotor Blade for the AH-1 Helicopter," Preprint No. 77.33.12, 33rd Annual National Forum of the American Helicopter Society, May 1977.

4 White, M.L., "Design and Fabrication of an Improved Performance, Low Cost, Composite Main Rotor Blade for the Cobra Helicopter," 22nd National SAMPE Symposium, April 1977, pp 511- 522.

5. Phillips, N. & Covington, C.E., "The 214 Fiberglass Blade - Design for Inspectability," Preprint No. 78-37, 34th Annual National Forum of the American Helicopter Society, May 1978.

6. Sanders, L.R., "Braiding - A Mechanical Means of Composite Fabrication," SAMPE Quarterly, January 2977, pp 34-44.

7. Post, R.J., "Braiding Composites - Adapting the Process for the Mass Production of Aerospace Components," 22nd National SAMPE Symposium, April 1977, pp 227-237.

8. Hardersen, C. & Blackburn, W., "Preliminary Design Study of a Composite Main Rotor Blade for the OH-58 Helicopter," USARTL-TR-78-29A, Fort Eustis, VA., September 1978.

9. "Advanced Composites Design Guide," Rockwell International Corporation, Air Force Flight Dynamics Laboratory, Air Force Systems Command, Wright-Patterson Air Force Base, Ohio, 1975.

10. Ashton, J.E., Halpin, J.C., and Petit, P.H., "Primer on Composite Materials: Analysis," Stamford, Connecticut, Technomic Publishing Co., Inc., 1969.

11. "Plastics for Aerospace Vehicles," Part 1, Reinforced Plastics, MIL-HDBK-17A, U.S. Government Printing Office, Washington, D.C., January 1971.

12. Stratton, W.K., "Evaluation of Dupont's High Modulus Organic Fiber PRD 49 Type I," Presented at 16th National SAMPE Symposium, April 22, 1971, Anaheim, California.

13. Hardersen, C., Blackburn, W., "Preliminary Design Study of a Composite Main Rotor Blade for the OH-58 Helicopter, Volume 1," Kaman Aerospace Corporation; USARTL-TR-78-29A, Applied Technology Laboratory, U.S. Army Research Technology Laboratories (AVRADCOM), Ft. Eustis, VA., September 1978.

14. Royal Aeronautical Society, Engineering Sciences Data, Vol. 8, Item 17015 "Buckling of Thin Flat Orthotropic Plates under Uniaxial Compression," London, Sept. 1971.

APPENDIX A

STRUCTURAL ANALYSIS

SUMMARY

Table A-1 presents the minimum margins of safety for the KA 757 braided blade between blade stations 80 and 180. Figures A-1, A-2, and A-3 compare the edgewise, torsional, and flatwise stiffnesses of the KA 757 blade to those of the standard blade. These data show adequate strength and appropriate stiffnesses for the KA 757 blade.

TABLE A-1. MINIMUM MARGINS OF SAFETY

Location/Type of Failure	M.S.
UPPER SURFACE	
Tension, Ultimate	+ .86
Compression, Ultimate	N.A. (tension only)
Shear, Ultimate	+4.62
Fatigue	+1.57
LOWER SURFACE	
Tension, Ultimate	+1.45
Compression, Ultimate	+ .16
Shear, Ultimate	+4.62
Fatigue	+3.12

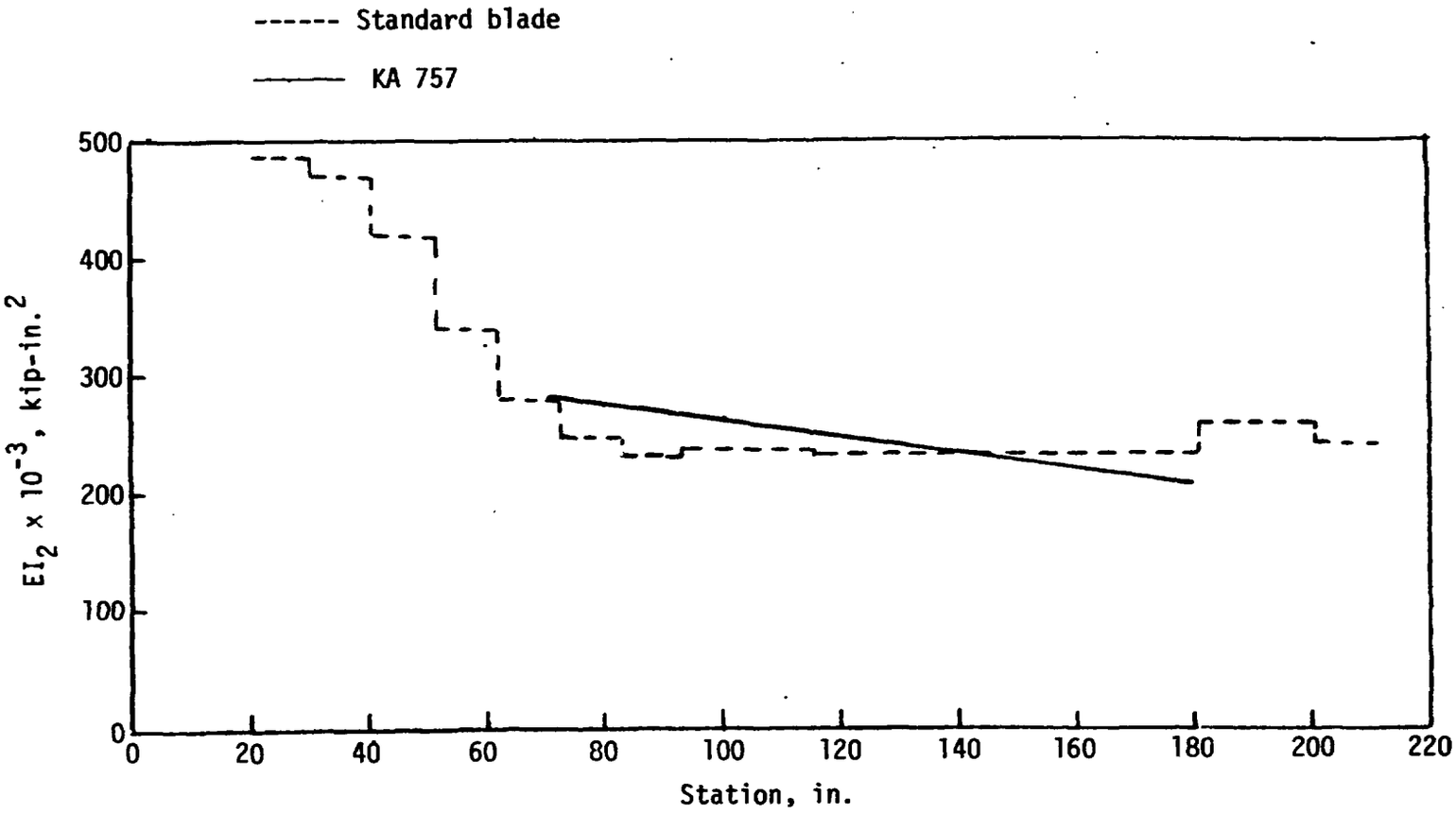

Figure A-1. Inplane Stiffness (EI_i) versus Blade Station.

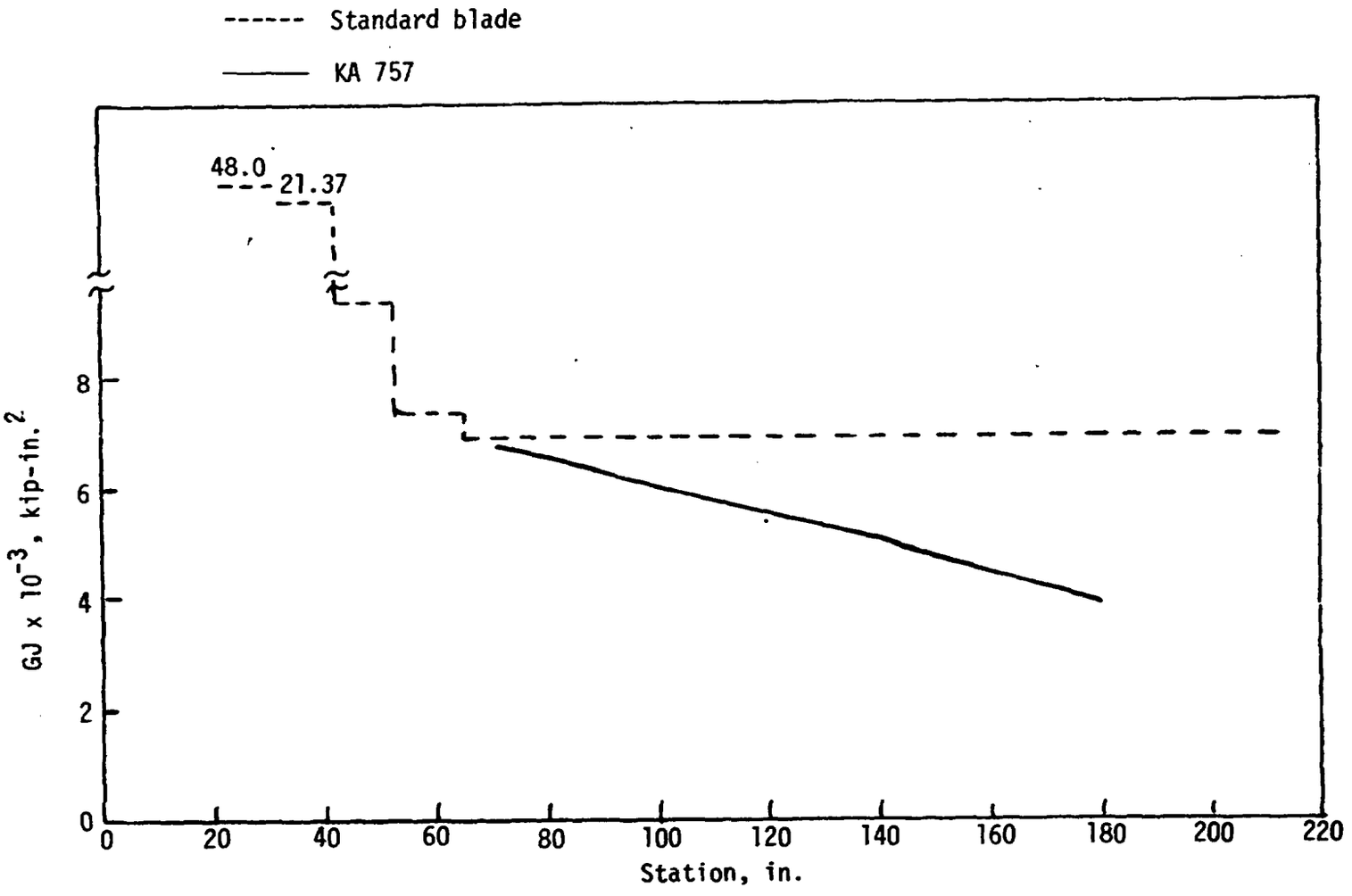

Figure A-2. Torsional Stiffness (GJ) versus Blade Station.

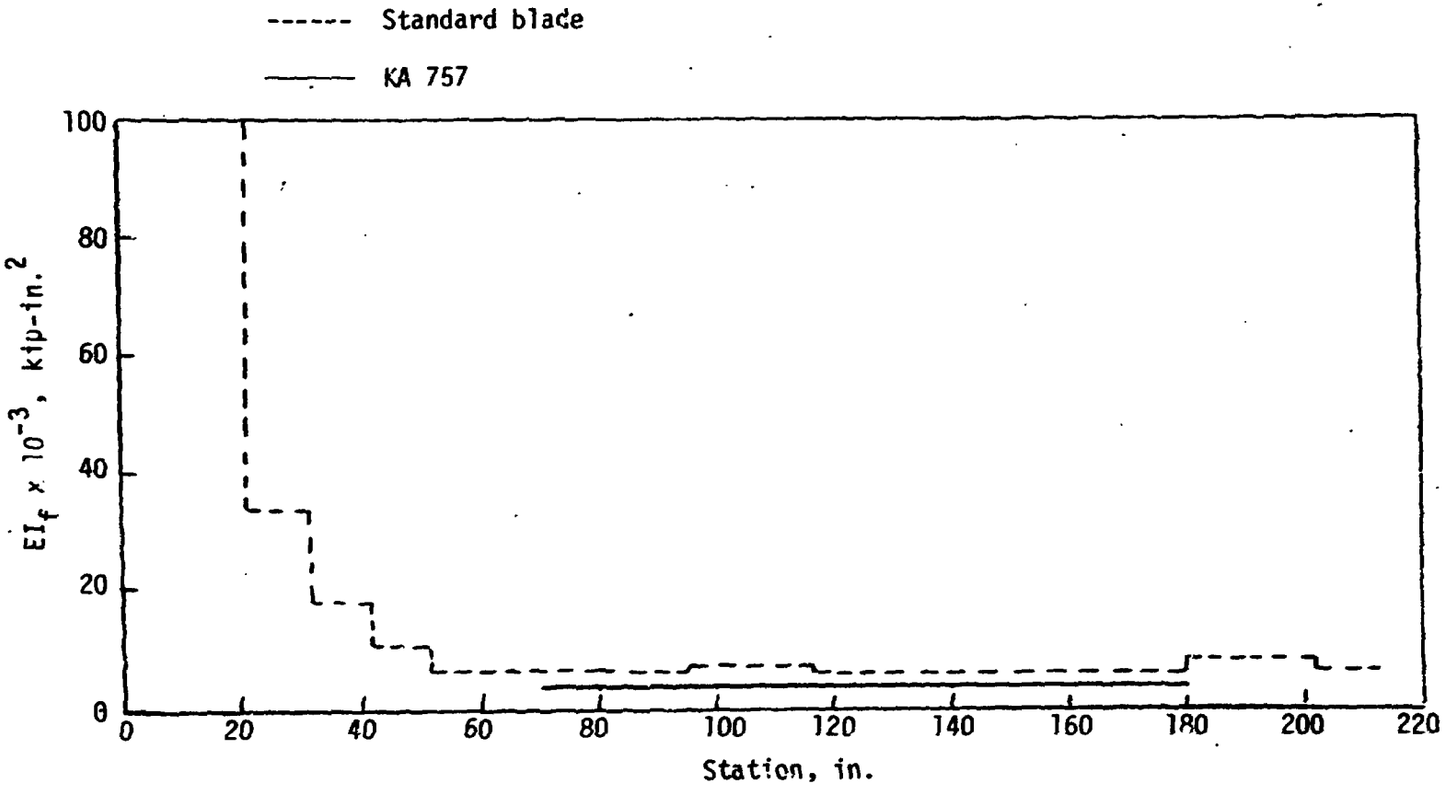

Figure A-3. Flatwise Stiffness (EI_f) versus Blade Station.

INTRODUCTION

This appendix presents:

1. Material properties and allowable stresses.
2. Design conditions
3. Stiffness and Strength Analyses

Throughout this appendix, the units of length and force are inches and kips, respectively.

The following notation is used:

Symbols:

α = orientation angle
β = orientation angle
ε = normal strain
γ = shear strain
ν = Poisson's ratio
σ = normal stress
τ = shear stress
E = modulus of elasticity
F = strength or force
g = acceleration of gravity
G = shear modulus
M = moment
V = shear

Subscripts and Superscripts:

cr = critical
cu = compression, ultimate
f = flatwise
i = inplane
su = shear, ultimate
tu = tension, ultimate
x, y = reference axes for laminate
1, 2 = reference axes for individual lamina
X, Y = reference axes for coordinates, loads, and stresses

Double subscripts used with moduli, Poisson's ratios, stresses, and strains correspond to conventional engineering usage.

MATERIAL PROPERTIES

The following material properties were used in the structural analyses:

1. Kevlar 49/Epoxy, Fiber-Resin System, Inplane Static Properties

E_{11}	= 10100 ksi	ν	= .34
E_{22}	= 800 ksi		
G_{12}	= 300 ksi		
F_{11}^{tu}	= 149 ksi	ε_{11}^{tu}	= .01475
F_{11}^{cu}	= -35 ksi	ε_{11}^{cu}	= -.00347
F_{22}^{tu}	= 3.5 ksi	ε_{22}^{tu}	= .00437
F_{22}^{cu}	= -17.5 ksi	ε_{22}^{cu}	= -.02187
F_{12}^{su}	= ±7.0 ksi	γ_{12}^{su}	= ±.02333

The above properties correspond to a unidirectional laminate with a fiber volume of 55 percent tested in the wet condition at room temperature. These properties were derived from tests reported in Reference 9 (for the dry condition) using the following reductions: 12.5 percent for the compressive strengths, and 19.5 percent for the shear strength.

The braiding process deposits layers of Kevlar fibers. Each layer consists of a closed, spiral pattern of fibers, half of which are oriented at a + angle, the others at a - angle relative to the longitudinal axis, x, of the mandrel. The angle and thickness of each layer depend upon the speed of traverse of the mandrel relative to the speed of rotation of the braider, the perimeter of the mandrel, the number of strands being braided, and the number of fibers in each strand. In the KA 757 blade, two speeds of traverse are used to produce a system ± α and ± β orientations at each station. At inboard stations (below station 70) additional fibers oriented at 0 degrees to the axis of the mandrel are inserted at the mid-thickness position. Figure A-4 shows the resulting orientations.

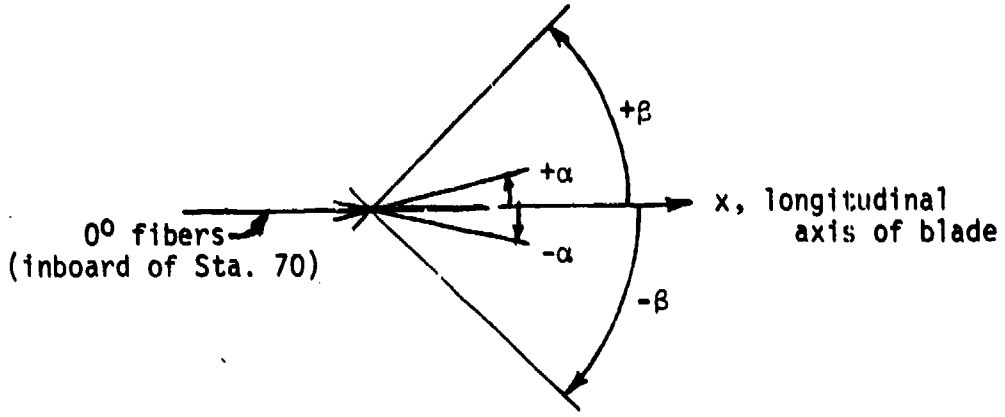

Figure A-4. Orientation of Fibers.

Figures A-5 and A-6 show the braid angles and spar wall thicknesses which are produced in the KA 757 blade when 7100 denier Kevlar is used with a 96 cop braiding machine and a fiber volume of 55%.

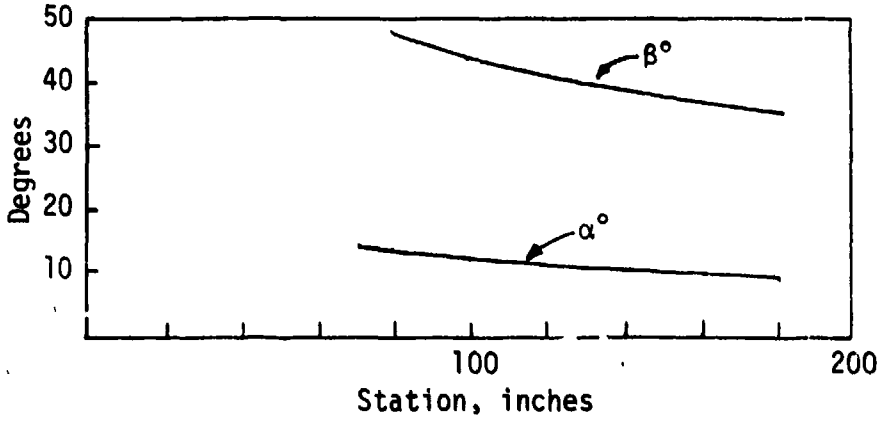

Figure A-5. Braid Angle Versus Blade Station.

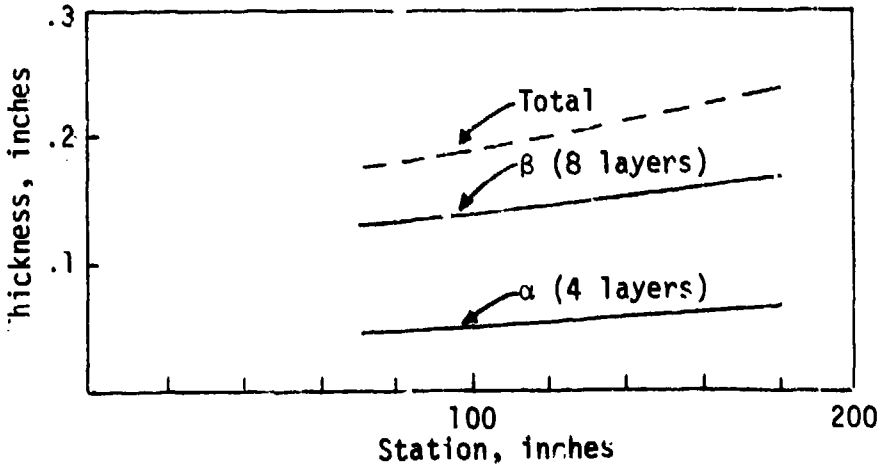

Figure A-6. Spar Thickness Versus Blade Station.

The elastic stiffness and strength properties for such laminates were calculated using plane stress, orthotropic material, lamination theory, and the maximum strain failure criteria. The calculations followed the composite theory presented in References 10 and 11. The Kaman computer program CMAB (Composite Materials Analysis Version B) was used. Table A-2 shows typical results, in this example for a Kevlar 49/epoxy laminate that occurs at station 80 of the KA 757 blade. The output includes terms (A, B, D, A', etc.) of the laminate consecutive equations as defined in Reference 2, conventional engineering moduli (E_x, E_y, G), and the stresses, strains, and margins of safety of each ply of the laminate for simple tension, compression and shear loadings. The load applied in each simple loading produced an average stress of 1 ksi. For such unit loadings, the allowable stress numerically equals the margin of safety (M.S.) + 1, as shown below:

$$\text{M.S.} = \frac{\text{allowable stress}}{\text{actual stress}} - 1$$

$$\text{allowable stress} = (\text{M.S.} + 1)(\text{actual stress} = 1)$$

Figure A-7 summarizes the calculated static strength of the spar laminate versus blade station for the KA-757 blade. These calculated strengths are conservative estimates because they correspond to the first failure of an individual ply, which is typically lower than the failure strength observed in tests.

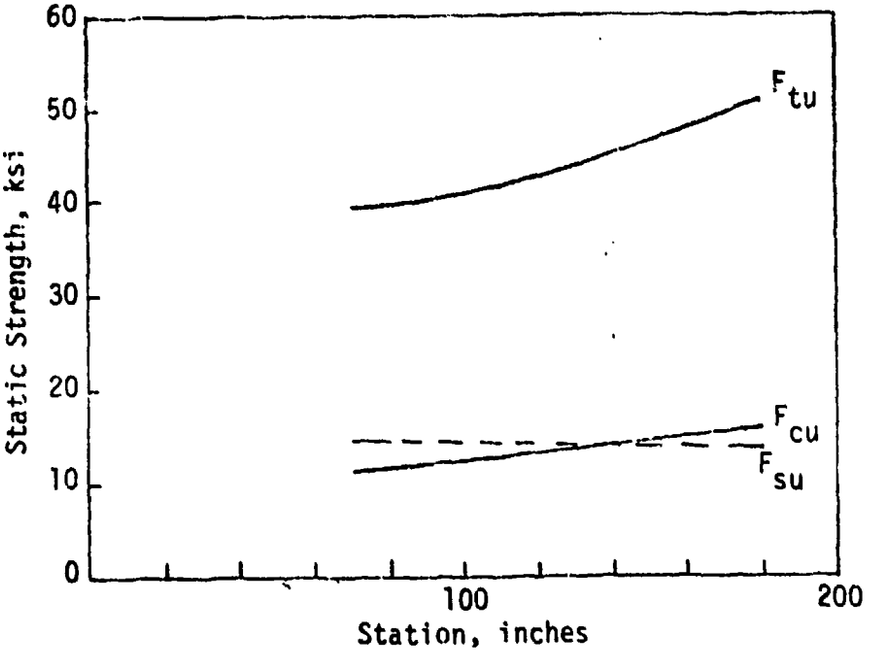

Figure A-7. Calculated Static Strength of Spar Laminate Versus Blade Station.

TABLE A-2. LAMINATE ANALYSIS FOR KEVLAR-49/EPOXY WITH ±46° AND ±13° ORIENTATION

PROG...CMAB
5/21/79

KEVLAR T=.183 . 328 AT +-46. .0472 AT +-13

MAT.	ALLOWABLE STRESS, UNIAXIAL 11	11	22	22	12	12	MODULI E11	E22	G	NU12
27	-35.0	149.	-17.5	3.50	-7.00	7.00	10100.	803.	330.	0.340

LAMINA	1	2	3	4	5	6	7	8	9	10	11	12	13	14	15
	16	7	18	19	20	21	22	23	24						
MATERIAL	27	7	27	27	27	27	27	27	27	27	27	27	27	27	27
	27	7	27	27	27	27	27	27	27						
THICKNESS	0.0084	0.0084	0.0084	0.0084	0.0059	0.0059	0.0059	0.0059	0.0084	0.0084	0.0084	0.0084	0.0084	0.0084	0.0084
	0.0084	0.0059	0.0059	0.0059	0.0059	0.0084	0.0084	0.0084	0.0084						
ANGLE	46.	46.	46.	-46.	13.	-13.	13.	-13.	45.	-45.	46.	-46.	-46.	46.	-46.
	46.	13.	13.	-13.	13.	-46.	46.	-46.	45.						

A B
B D

8.445E 02	3.813E 02	3.052E-05	4.864E-05	2.193E-05	1.907E-06
3.813E 02	4.903E 02	3.052E-05	2.193E-05	2.670E-05	2.851E-06
3.052E-05	3.052E-05	3.859E 02	1.907E-06	2.861E-06	2.193E-05
4.854E-05	2.193E-05	1.907E-06	2.132E 00	1.104E 00	1.406E-01
2.193E-05	2.670E-05	2.861E-06	1.104E 00	1.424E 00	1.259E-01
1.907E-06	2.861E-06	2.193E-05	1.406E-01	1.258E-01	1.117E 00

A' B'
C' D'

1.825E-03	-1.419E-03	-3.209E-11	-4.398E-08	3.240E-08	2.494E-09
-1.419E-03	3.143E-03	-1.363E-10	3.228E-08	-6.189E-08	-2.719E-09
-3.209E-11	-1.363E-10	2.591E-03	2.350E-09	-2.533E-09	-5.089E-08
-4.398E-08	3.228E-08	2.350E-09	7.852E-01	-6.064E-01	-3.052E-02
3.240E-08	-6.189E-08	-2.533E-09	-6.064E-01	1.178E 00	-5.634E-02
2.494E-09	-2.719E-09	-5.089E-08	-3.052E-02	-5.634E-02	9.054E-01

A* B*
C* D*

1.825E-03	-1.419E-03	-3.209E-11	-5.763E-08	-2.133E-09	5.795E-10
-1.419E-03	3.143E-03	-1.363E-10	8.379E-11	-5.280E-08	-6.286E-09
-3.209E-11	-1.363E-10	2.591E-03	-4.942E-09	-7.413E-09	-5.683E-08
5.763E-08	-8.384E-11	4.942E-09	2.132E 00	1.104E 00	1.406E-01
2.133E-09	5.280E-08	7.413E-09	1.104E 00	1.424E 00	1.259E-01
-5.795E-10	6.286E-09	5.683E-08	1.406E-01	1.258E-01	1.117E 00

LAMINATE PROPERTIE	EX	EY	G
K'S UNRESTRAINE	3017.	1752.	2125.
K'S = 0	3017.	1752.	2125.

TABLE A-2 (CONTINUED)

BEHAVIOR FOR NX= 0.180 NY= 0.0 NXY= 0.0 KX= 0.0 KY= 0.3 KXY= 0.0

LAM. NO.	STRESSES X	Y	XY	STRAINS 11	22	12	11	22	12	M.S. 11	22	12	MIN.
24	0.3	-0.0	0.1	0.3	0.0	-0.2	0.000026	0.000047	-0.000584	99.00	92.62	38.98	38.98
23	0.3	-0.0	-0.1	0.3	0.0	0.2	0.000026	0.000047	0.000584	99.00	92.62	38.98	38.98

etc.

9	0.3	-0.0	0.1	0.3	0.0	-0.2	0.000026	0.000047	-0.000584	99.00	92.62	38.98	38.98
8	2.9	0.0	-0.6	3.0	-0.1	0.1	0.000299	-0.000226	0.000255	48.35	95.83	90.15	48.35
7	2.9	0.0	0.6	3.0	-0.1	-0.1	0.000299	-0.000226	-0.000256	48.35	95.83	90.15	48.35
6	2.9	0.0	-0.6	3.0	-0.1	0.1	0.000299	-0.000226	0.000256	48.35	95.83	90.15	48.35
5	2.9	0.0	0.6	3.0	-0.1	-0.1	0.000299	-0.000226	-0.000255	48.35	95.83	90.15	48.35
4	0.3	-0.0	-0.1	0.3	0.0	0.2	0.000026	0.000047	0.000584	99.00	92.62	38.98	38.98
3	0.3	-0.0	0.1	0.3	0.0	-0.2	0.000026	0.000047	-0.000584	99.00	92.62	38.98	38.98
2	0.3	-0.0	-0.1	0.3	0.0	0.2	0.000026	0.000047	0.000584	99.00	92.62	38.98	38.98
1	0.3	-0.0	0.1	0.3	0.0	-0.2	0.000026	0.000047	-0.000584	99.00	92.62	38.98	38.98
ALL	1.0	0.0	0.0				0.000328	-0.000255	-0.000000				

BEHAVIOR FOR NX= 0.180 NY= 0.0 NXY= 0.0 KX= 0.0 KY= 0.3 KXY= 0.0

LAM. NO.	STRESSES X	Y	XY	STRAINS 11	22	12	11	22	12	M.S. 11	22	12	MIN.
24	-0.3	0.0	-0.1	-0.3	-0.0	0.2	-0.000026	-0.000047	0.000584	99.00	99.00	38.98	38.98
23	-0.3	0.0	0.1	-0.3	-0.0	-0.2	-0.000026	-0.000047	-0.000584	99.00	99.00	38.98	38.98

etc.

9	-0.3	0.0	-0.1	-0.3	-0.0	0.2	-0.000026	-0.000047	0.000584	99.00	99.00	38.98	38.98
8	-2.9	-0.0	0.6	-3.0	0.1	-0.1	-0.000299	0.000226	-0.000256	10.59	18.37	90.15	10.59
7	-2.9	-0.0	-0.6	-3.0	0.1	0.1	-0.000299	0.000226	0.000256	10.59	18.37	90.15	10.59
6	-2.9	-0.0	0.6	-3.0	0.1	-0.1	-0.000299	0.000226	-0.000256	10.59	18.37	90.15	10.59
5	-2.9	-0.0	-0.6	-3.0	0.1	0.1	-0.000299	0.000226	0.000256	10.59	18.37	90.15	10.59
4	-0.3	0.0	0.1	-0.3	-0.0	-0.2	-0.000026	-0.000047	-0.000584	99.00	99.00	38.98	38.98
3	-0.3	0.0	-0.1	-0.3	-0.0	0.2	-0.000026	-0.000047	0.000584	99.00	99.00	38.98	38.98
2	-0.3	0.0	0.1	-0.3	-0.0	-0.2	-0.000026	-0.000047	-0.000584	99.00	99.00	38.98	38.98
1	-0.3	0.0	-0.1	-0.3	-0.0	0.2	-0.000026	-0.000047	0.000584	99.00	99.00	38.98	38.98
ALL	-1.0	0.0	0.0				-0.000328	0.000255	0.000000				10.59

BEHAVIOR FOR NX= 0.0 NY= 0.0 NXY= 0.180 KX= 0.0 KY= 0.0 KXY= 0.0

LAM. NO.	STRESSES X	Y	XY	STRAINS 11	22	12	11	22	12	M.S. 11	22	12	MIN.
24	1.1	1.1	1.2	2.3	-0.1	-0.0	0.000233	-0.000233	-0.000016	62.30	92.86	99.00	62.30
23	-1.1	-1.1	1.2	-2.3	0.1	-0.0	-0.000233	0.000233	-0.000016	13.87	17.77	99.00	13.87

etc.

9	1.1	1.1	1.2	2.3	-0.1	-0.0	0.000233	-0.000233	-0.000016	62.30	92.86	99.00	62.30
8	-0.9	-0.1	0.3	-1.0	0.1	0.1	-0.000102	0.000102	0.000419	32.90	41.79	54.66	32.90
7	0.9	0.1	0.3	1.0	-0.1	0.1	0.000102	-0.000102	0.000419	99.00	99.00	54.66	54.66
6	-0.9	-0.1	0.3	-1.0	0.1	0.1	-0.000102	0.000102	0.000419	32.90	41.79	54.66	32.90
5	0.9	0.1	0.3	1.0	-0.1	0.1	0.000102	-0.000102	0.000419	99.00	99.00	54.66	54.66
4	-1.1	-1.1	1.2	-2.3	0.1	-0.0	-0.000233	0.000233	-0.000016	13.87	17.77	99.00	13.87
3	1.1	1.1	1.2	2.3	-0.1	-0.0	0.000233	-0.000233	-0.000016	62.30	92.86	99.00	62.30
2	-1.1	-1.1	1.2	-2.3	0.1	-0.0	-0.000233	0.000233	-0.000016	13.87	17.77	99.00	13.87
1	1.1	1.1	1.2	2.3	-0.1	-0.0	0.000233	-0.000233	-0.000016	62.30	92.86	99.00	62.30
ALL	0.0	0.0	1.0				-0.000000	-0.000000	0.000466				13.87

Figure A-8 summarizes the calculated elastic moduli E and G of the spar laminate versus blade station.

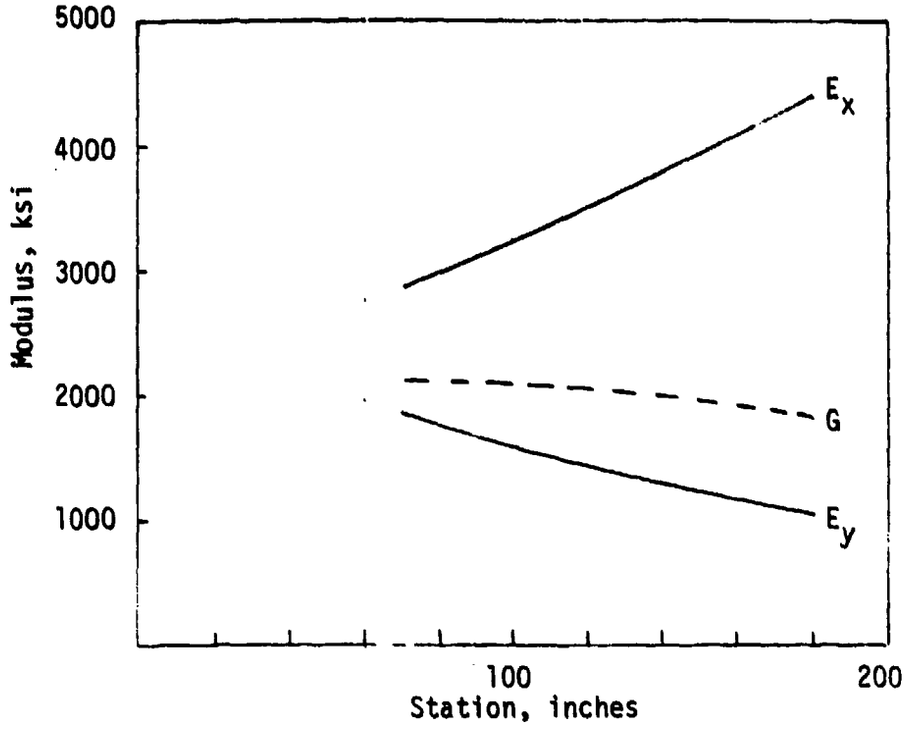

Figure A-8. Calculated Elastic Moduli of Spar Laminate Versus Blade Station.

2. Kevlar 49/Epoxy, Fiber-Resin System, Inplane Fatigue Properties

Figure A-9 shows the calculated fatigue strength of the laminate at a typical station, in this example, station 80.

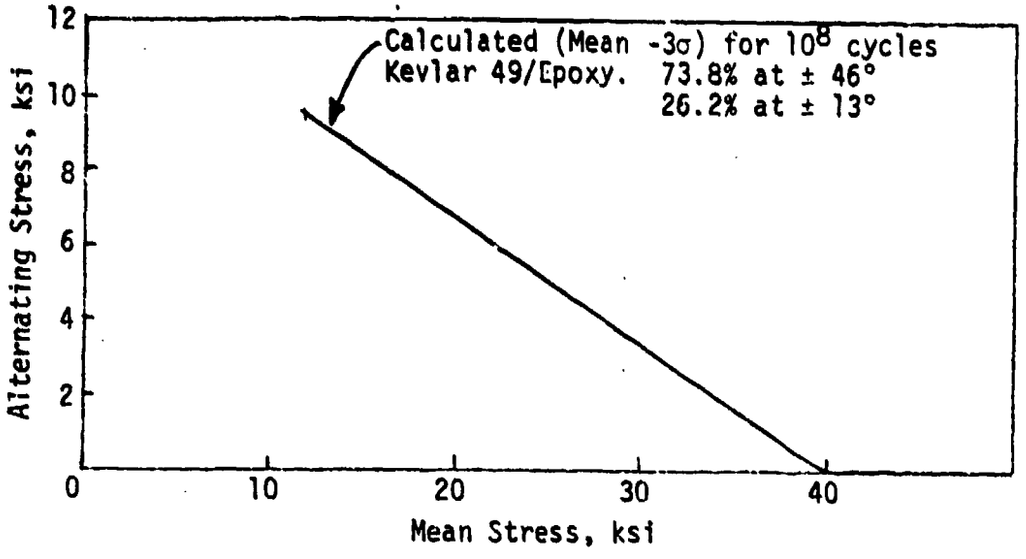

Figure A-9. Fatigue Strength for Laminate at Station 80.

Figure A-9 was calculated in the following manner:

a. It was theorized that in tension-tension fatigue (Stress Ratio > 0) the fatigue strength of angle ply laminates is dominated by the resin and is directly related to the shearing strain along the 1-2 axis of an individual layer.

b. The critical shear strain to cause fatigue failure was deduced from tests of $\pm 45^0$ laminates reported in Reference 12. Figure A-10 shows the data for these tests. Using lamination theory (CMAB program) it was found that the 3-σ reduced alternating stress at 10^8 cycles, ±3.36 ksi in Figure A-10, corresponds to an alternating shear strain in the 1-2 direction of .005601. Thus, the critical shear strain is .005601.

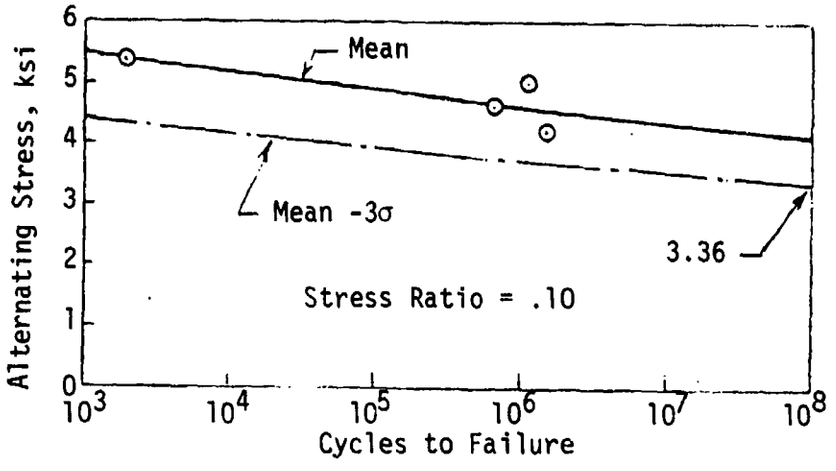

Figure A-10. S-N Curve for Kevlar 49/Epoxy for $\pm 45^{o}$ Laminate.

c. Table A-2 presents a lamination theory analysis of the laminate at station 80. It shows that for N_x = .180, corresponding to an axial load of 1 ksi, the maximum shearing strains in the 1-2 direction is .000584. Thus, the alternating stress required to produce the critical shear strain - .005601/.000584 - 9.59 ksi. With the stress ratio of .1 the corresponding mean stress is 11.72 ksi. These values establish the left-hand of the strength line shown in Figure A-9. The right-hand end is the static strength, 39.94 ksi, also from Table A-2.

3. E-Glass/Epoxy, Fiber-Resin System

The nose block consists primarily of unidirectional E-glass oriented spanwise. The elastic modulus for the noseblock is taken herein as

$$E_{11} = 5000 \text{ ksi}$$

DESIGN CONDITIONS

Figure A-11 shows the coordinate system used herein to describe the loading conditions and the coordinates for subsequent analysis. Moments follow the conventional left-hand rule. All forces and moments act upon the inboard face, shaded.

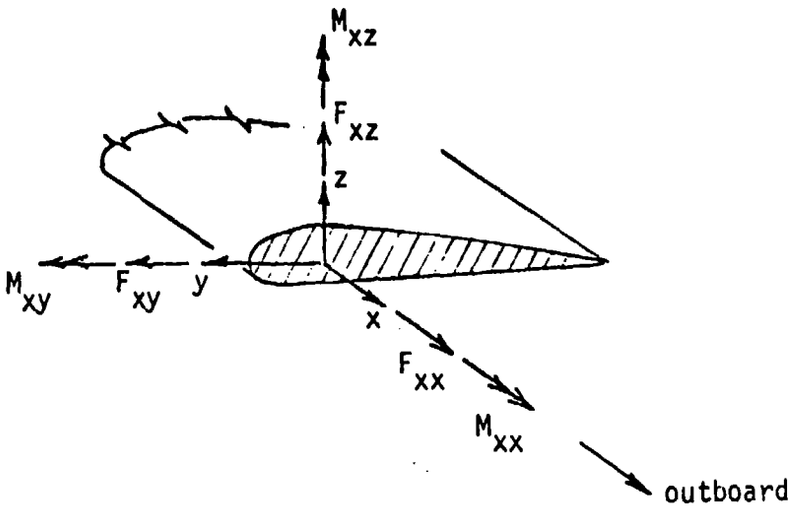

Figure A-11. Coordinate System.

In the region from station 80 outboard, station 80 experiences the highest loadings and the corresponding lower margins of safety. Margins of safety are calculated at station 80 for the following six design conditions:

1. Maximum Tension in Upper Surface, Case 4.14

An ultimate condition corresponding to Condition III limit x 1.5 + centrifugal force at 411 RPM limit x 1.5 (from Reference 13).

$$F_{xx} = 66.22 \text{ kips, ultimate.}$$

2. Maximum Tension in Lower Surface, Case 4.20

An ultimate condition corresponding to the flatwise moments from Conditions I and IX limit x 1.5 + flatwise shears limit x 1.5 + centrifugal force at 411 RPM limit x 1.5 (all from Reference 13).

$$F_{xx} = 66.22 \text{ kips, ultimate}$$

$$F_{xy} = .36 \text{ kips, ultimate}$$

$$M_{xy} = -6.75 \text{ in.-kips, ultimate}$$

3. Maximum Compression in Lower Surface, Case 4.12

An ultimate condition corresponding to a 4-g static droop.

F_{xz} = -.233 kips, ultimate

F_{xy} = 17.7 in.-kips, ultimate

The static droop shears and moment correspond to an assumed blade weight distribution similar to that in Reference 5. The following calculation presents the 4-g static droop loads, shears and moments for the blade.

Station	0	20	40	60	80	100	120	140	160	180	200	in.
4-g wt.		.108	.0248	.0188	.0184	.0172	.0164	.0848	.0356	.036	.0432	kip
V	.4032	.2952	.2704	.2516	.2332	.2160	.1996	.1148	.0792	.0432		kip
M	42.13	34.06	28.16	22.75	17.72	13.06	8.74	4.74	2.45	.864	0	in.-kip

4. Maximum Shear in Upper and Lower Surface, Case 4.16

An ultimate condition corresponding to limit pitching moment x 1.5 (from Reference 5).

M_{xx} = 7.16 in.-kips, ultimate

5. Alternating Stresses in Upper and Lower Surfaces, Case 4.17

A conservative fatigue condition corresponding to a gross weight of 3000 lbs, a density altitude of 6000 ft., a rotor speed of 347 rpm, a velocity of 130 kts, and a c.g. at fuselage station 112.1 in. (from Reference 5).

M_{xy} = ±2.6 in.-kips, fatigue alternating

6. Mean Stress in Upper and Lower Surfaces, Case 4.18

The mean loads corresponding to the alternating load of condition 5 above + centrifugal force at 354 RPM (from Reference 5).

F_{xx} = 32.75 kips, fatigue steady

M_{xy} = -1.1 in.-kips, fatigue steady

STIFFNESSES, STRESSES, AND MARGINS OF SAFETY

The stiffnesses and stresses were computed using the Kaman SHELLD program which obtains a conventional beam and torsion solution in which plane sections remain plane and all closed shear cells rotate through the same angle. The effects of taper and differing moduli for elements of the cross section are included. Figure A-12 shows the idealized cross section. The circled numbers correspond to "effective" stringer elements where the bending area is concentrated. The non-circled numbers identify "skin" elements.

Table A-3 shows the SHELLD results for the stiffness analysis and stress analysis for each of the design conditions, all at station 80. Similar stiffness analyses were performed at other stations to provide the data shown in Figures A-1, A-2, and A-3. The margins of safety shown in Table A-3 are based upon ficticious allowables of ±100 ksi and thus can be ignored. The actual margins of safety are calculated as follows:

1. Maximum Tension in Upper Surface, Case 4.14

From Table A-3, the maximum tensile stress = 21.48 ksi at element 9.
From Table A-2, the allowable tensile stress - 39.94 ksi.

$$\text{M.S.} = \frac{39.98}{21.48} - 1 = \underline{+.86} \text{ (ult)}$$

2. Maximum Tension in Lower Surface, Case 4.20

From Table A-3, the maximum tensile stress = 16.28 ksi at element 4.

$$\text{M.S.} = \frac{39.98}{16.28} = \underline{+1.45} \text{ (ult)}$$

3. Maximum Compression in Lower Surface, Case 4.12

From Table A-3, the maximum compressive stress = -9.9 ksi at element 2.
From Table A-2, the allowable compressive stress is -11.55 ksi.

$$\text{M.S.} = \frac{-11.59}{-9.97} - 1 = \underline{+.16} \text{ (ult)}$$

Another possible mode of failure in compression is instability or buckling. The margin of safety for buckling is shown to be high by the following conservative analysis which considers the lower surface of the spar to be a simply supported flat plate of long length. The effective width b the plate is taken as 75% of the free span as shown in Figure A-13.

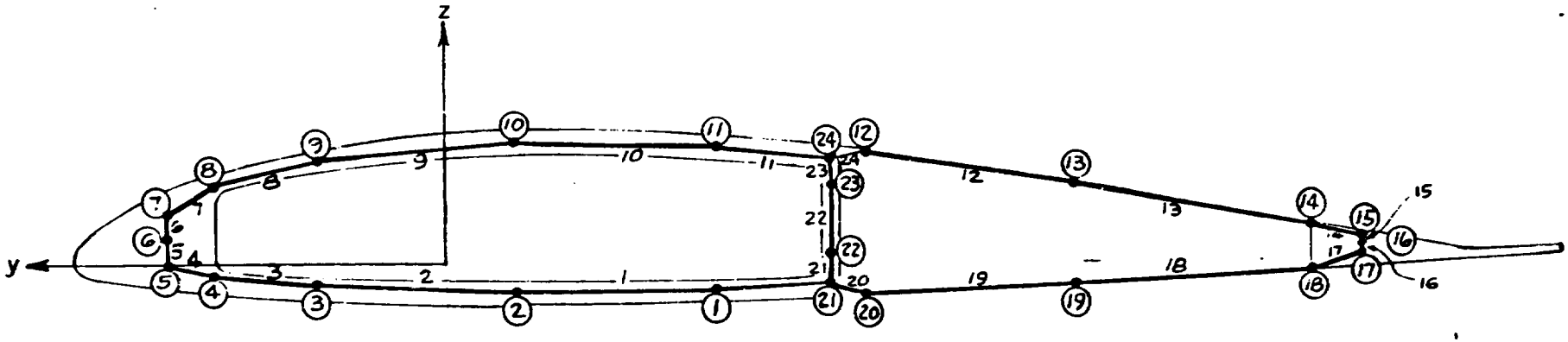

At Station 36.50

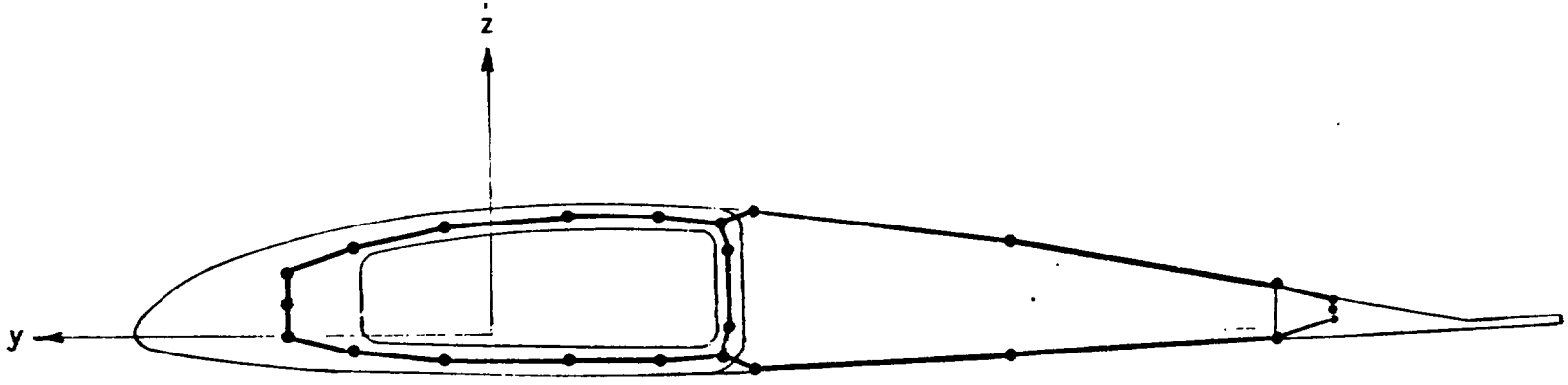

At Station 179.92

Figure A-12. Blade Cross-Section Model for Structural Analyses.

TABLE A-3 ANALYSIS OF STATION 80

CH-53 BRAILEE BLADE RUN 3 4/26/79 SHELL-D USES
UNIT LOAD CASES X 10 INCH-KIP SYSTEM

CASE 4.00
INPUT DATA

BASIC MODULI
STRINGER E = 1000.
SKIN G = 1000.

ELEM.	STATION 80.00 COORDINATES Y	Z	STATION 36.50 COORDINATES Y	Z	COMP. AREA	TENS. AREA	CRITICAL STRESS COMP.	TENS.	REL. MOD.	SKIN THICK.	SKIN MOD.	ASF	CF	TF
1	-2.34	-0.285	-2.70	-0.300	0.0000	0.2341	-100.00	100.00	3.02	0.1800	2120.	0.0000	0.0	0.500
2	-3.70	-0.272	-0.70	-0.290	0.0000	0.3000	-100.00	100.00	3.02	0.1800	2120.	0.0000	0.0	0.500
3	1.00	-0.224	1.30	-0.230	0.0000	0.2436	-100.00	100.00	3.02	0.1800	2120.	0.0000	0.0	0.500
4	2.00	-0.130	2.35	-0.125	0.0000	0.2414	-100.00	100.00	3.02	0.5920	1000.	0.0000	0.0	0.500
5	2.50	-0.015	2.80	-0.020	0.0000	0.2499	-100.00	100.00	5.00	0.5920	1000.	0.0000	0.0	0.500
6	2.50	0.321	2.80	0.350	0.0000	0.1979	-100.00	100.00	5.00	0.5920	1000.	0.0000	0.0	0.500
7	2.50	0.654	2.80	0.690	0.0000	0.2489	-100.00	100.00	5.00	0.5920	1000.	0.0000	0.0	0.500
8	2.00	0.766	2.35	0.760	0.0000	0.2433	-100.00	100.00	3.02	0.1800	2120.	0.0000	0.0	0.500
9	1.00	1.002	1.30	1.025	0.0000	0.2462	-100.00	100.00	3.02	0.1800	2120.	0.0000	0.0	0.500
10	-0.70	1.155	-0.70	1.210	0.0000	0.3006	-100.00	100.00	3.02	0.1800	2120.	0.0000	0.0	0.500
11	-2.34	1.118	-2.70	1.160	0.0000	0.2343	-100.00	100.00	3.02	0.1800	2120.	0.0000	0.0	0.500
12	-3.63	1.105	-4.20	1.120	0.0000	0.0216	-100.00	100.00	2.70	0.0170	1056.	0.0000	0.0	0.500
13	-5.90	0.787	-6.32	0.790	0.0000	0.0391	-100.00	100.00	2.70	0.0170	1056.	0.0000	0.0	0.500
14	-8.17	0.366	-8.70	0.360	0.0000	0.0249	-100.00	100.00	2.70	0.0170	1056.	0.0000	0.0	0.500
15	-8.67	0.206	-9.70	0.200	0.1700	0.1700	-100.00	100.00	10.10	1.0000	300.	0.1700	0.0	0.0
16	-8.67	0.146	-9.20	0.140	0.0000	0.0000	-100.00	100.00	2.70	1.0000	300.	0.0000	0.0	0.0
17	-8.67	0.086	-9.20	0.080	0.1700	0.1700	-100.00	100.00	10.10	0.0170	1056.	0.1700	0.0	0.0
18	-6.17	-0.100	-8.70	-0.100	0.0000	0.0247	-100.00	100.00	2.70	0.0170	1056.	0.0000	0.0	0.500
19	-5.90	-0.230	-6.32	-0.230	0.0000	0.0386	-100.00	100.00	2.70	0.0170	1056.	0.0000	0.0	0.500
20	-3.63	-0.337	-4.20	-0.340	0.0000	0.0215	-100.00	100.00	2.70	0.0170	1056.	0.0000	0.0	0.500
21	-3.30	-0.207	-3.85	-0.210	0.0000	0.0899	-100.00	100.00	3.02	0.1800	2120.	0.0000	0.0	0.500
22	-3.33	0.067	-3.87	0.070	0.1200	0.1200	-100.00	100.00	3.02	0.1800	2120.	0.1200	0.0	0.0
23	-3.33	0.763	-3.87	0.780	0.1200	0.1200	-100.00	100.00	3.02	0.1800	2120.	0.1200	0.0	0.0
24	-3.30	1.019	-3.85	1.040	0.0000	0.0900	-100.00	100.00	3.02	0.0170	1056.	0.0000	0.0	0.500
25										0.1800	2120.			

SUMMARY OF PROPERTIES FOR THE TRANSFORMED SECTION

CENTROIDAL
IYZ = 4.561E 00 AREA = 14.817 ELASTIC CENTER BASIC MODULI
IYY = 3.341E 00 YCENT = -1.902 YEA = -0.584 E = 1000.
IZZ = 2.736E 02 ZCENT = 0.317 ZEA = 0.472 G = 1000.

PRINCIPAL CENTROIDAL AXES ARE CALLED 2-AXIS AND 3-AXIS

THETA = 0.97 DEG. ANGLE FROM Y-AXIS TO 2-AXIS (USING LEFT-HAND RULE ABOUT X-AXIS)

A1 = 14.8170 AREA
A2 = 0.7879 SHEAR-AREA FOR FORCE AT ELASTIC CENTER ALONG 2-AXIS
A3 = 0.4349 SHEAR-AREA FOR FORCE AT ELASTIC CENTER ALONG 3-AXIS

I1 = 6.514E 00 TORSIONAL STIFFNESS /G
I2 = 3.264E 00 I FOR BENDING ABOUT 2-AXIS
I3 = 2.737E 02 I FOR BENDING ABOUT 3-AXIS

TABLE A-3 (CONTINUED)

CH-58 BRAIDED BLADE — RUN 3 — 4/26/79

CASE 4.12
STA. 89.00

LOAD Y = -0.58
POINT Z = 0.47

MXX = 0.0 FXX = 0.0
MXY = 17.700 FXY = 0.0
MXZ = 0.0 FXZ = -0.233

NO.	AXIAL STRESS	M.S.	COMPONENTS OF FORCE X	Y	Z	SHEAR FLOW	SHEAR STRESS	SKIN FORCE COMP. Y	Z
1	-9.74	9.27	-2.279	-0.019	-0.001	0.026	0.14	0.047	-0.002
2	-9.27	9.03	-2.991	0.0	-0.001	-0.011	-0.06	0.012	-0.000
3	-9.65	9.37	-2.350	0.016	-0.000	-0.040	-0.22	-0.029	-0.002
4	-9.38	10.94	-2.022	0.016	0.000	-0.065	-0.11	-0.036	-0.006
5	-13.93	8.11	-2.745	0.019	-0.001	-0.098	-0.17	-0.016	-0.020
6	-1.88	52.09	-0.373	0.003	0.000	-0.102	-0.17	0.0	-0.034
7	7.13	13.02	1.775	-0.012	-0.001	-0.080	-0.14	0.020	-0.022
8	5.29	14.91	1.529	-0.012	0.000	-0.061	-0.34	0.051	-0.012
9	11.43	8.59	2.567	-0.018	-0.001	-0.030	-0.16	0.055	-0.009
10	13.39	6.47	4.027	0.0	-0.005	0.020	0.11	0.009	-0.013
11	13.22	6.56	3.098	0.026	-0.003	0.058	0.32	-0.044	-0.033
12	11.95	7.27	0.258	0.003	-0.000	0.006	0.36	-0.007	-0.031
13	7.83	11.78	0.316	0.004	-0.000	0.010	0.58	-0.018	-0.033
14	2.25	43.53	0.056	0.001	0.000	0.011	0.62	-0.014	-0.003
15	0.13	99.00	0.017	0.000	0.000	0.010	0.01	-0.003	-0.001
16	-0.85	99.00	-0.000	-0.000	-0.000	0.010	0.01	0.0	-0.001
17	-6.47	14.45	-1.100	-0.013	-0.000	-0.004	-0.24	-0.001	0.000
18	-4.54	20.86	-0.113	-0.001	0.0	-0.006	-0.33	-0.008	0.001
19	-7.76	13.17	-1.273	-0.003	0.0	-0.009	-0.53	-0.016	0.001
20	-9.15	9.53	-0.197	-0.003	-0.000	-0.011	-0.67	-0.012	-0.000
21	-9.21	11.20	-0.737	-0.009	-0.000	-0.074	-0.41	0.025	-0.013
22	-3.73	26.00	-0.444	-0.005	0.000	-0.080	-0.44	0.001	-0.038
23	7.70	11.59	0.923	0.011	-0.000	-0.068	-0.38	-0.001	-0.036
24	11.47	7.43	1.067	0.014	-0.001	0.003	0.17	-0.030	-0.011
25						0.054	0.30	0.0	0.0

X-TWIST = 0.000002326 RAD./IN.
Y-CURV. = 0.005420718 RAD./IN.
Z-CURV. = 0.000390345 RAD./IN.

CHECKS, MXX = 0.000 FXX = 0.000
MXY = 17.700 FXY = -0.000
MXZ = -0.000 FXZ = -0.233

CH-58 BRAIDED BLADE — RUN 3 — 4/26/79

CASE 4.14
STA. 80.00

LOAD Y = -0.58
POINT Z = 0.47

MXX = 0.0 FXX = 66.220
MXY = 0.0 FXY = 0.0
MXZ = 0.0 FXZ = 0.0

NO.	AXIAL STRESS	M.S.	COMPONENTS OF FORCE X	Y	Z	SHEAR FLOW	SHEAR STRESS	SKIN FORCE COMP. Y	Z
1	9.23	11.14	1.928	0.016	0.001	0.001	0.00	-0.000	0.000
2	9.69	9.32	2.909	0.0	0.001	0.004	0.02	0.004	0.000
3	11.49	7.70	2.798	-0.020	0.000	0.006	0.03	0.005	0.000
4	13.09	6.64	3.159	-0.025	-0.000	0.008	0.01	0.005	0.001
5	23.90	3.18	5.972	-0.042	0.002	0.010	0.02	0.002	0.002
6	28.42	2.52	5.624	-0.039	-0.001	0.010	0.02	0.0	0.003
7	32.91	2.04	8.191	-0.057	-0.007	0.008	0.01	-0.002	0.002
8	27.39	2.91	4.956	-0.040	0.001	0.006	0.03	-0.005	0.001
9	21.43	3.66	5.288	-0.037	-0.003	0.003	0.02	-0.005	0.001
10	21.32	3.69	6.409	0.0	-0.008	-0.002	-0.01	-0.001	0.000
11	19.65	4.09	4.607	0.039	-0.004	-0.005	-0.03	0.004	0.000
12	16.53	5.05	0.356	0.005	-0.000	-0.002	-0.10	0.002	0.000
13	12.61	6.93	0.493	0.006	-0.000	-0.002	-0.11	0.004	0.001
14	7.73	11.84	0.194	0.002	0.000	-0.002	-0.11	0.003	0.001
15	23.39	3.28	3.976	0.049	0.001	-0.001	-0.00	0.000	0.000
16	5.82	26.20	0.000	0.000	0.000	-0.001	-0.00	0.0	0.000
17	21.12	3.97	3.420	0.042	0.000	0.002	0.09	0.003	-0.000
18	4.39	21.76	0.109	0.001	0.0	0.002	0.10	0.002	-0.000
19	5.23	18.23	0.201	0.002	0.0	0.002	0.12	0.004	-0.000
20	5.03	15.60	0.130	0.002	0.000	0.002	0.13	0.003	0.000
21	8.07	11.39	0.726	0.009	0.000	0.005	0.03	-0.001	0.001
22	13.24	8.73	1.233	0.015	-0.000	0.005	0.03	-0.000	0.003
23	15.95	6.27	1.914	0.024	-0.001	0.005	0.03	0.000	0.002
24	19.05	4.54	1.624	0.021	-0.001	-0.001	-0.08	0.003	0.001
25						-0.002	-0.01	0.0	0.0

X-TWIST = 0.000003216 RAD./IN.
Y-CURV. = 0.002697841 RAD./IN.
Z-CURV. = -0.000273995 RAD./IN.

CHECKS, MXX = -0.000 FXX = 66.220
MXY = 0.000 FXY = 0.000
MXZ = 0.000 FXZ = -0.000

TABLE A-3 (CONTINUED)

OH-58 BRAIDED BLADE — RUN 3 — 4/26/79

CASE 4.16 — LOAD Y = -0.58 — MXX = 7.150 — FXX = 0.0
STA. 90.00 — POINT Z = 0.47 — MXY = 0.0 — FXY = 0.0
MXZ = 0.0 — FXZ = 0.0

NO.	AXIAL STRESS	M.S.	COMPONENTS OF FORCE X	Y	Z	SHEAR FLOW	SHEAR STRESS	SKIN FORCE COMP. Y	Z
1	0.0	99.00	0.0	0.0	0.0	0.475	2.64	0.617	-0.015
2	0.0	99.00	0.0	0.0	0.0	0.475	2.64	0.791	0.014
3	0.0	99.00	0.0	0.0	0.0	0.475	2.64	0.641	0.134
4	0.0	99.00	0.0	0.0	0.0	0.475	0.80	0.356	0.050
5	0.0	99.00	0.0	0.0	0.0	0.475	0.80	0.118	0.137
6	0.0	99.00	0.0	0.0	0.0	0.475	0.80	0.0	0.159
7	0.0	99.00	0.0	0.0	0.0	0.475	0.80	-0.118	0.106
8	0.0	99.00	0.0	0.0	0.0	0.475	2.64	-0.356	0.093
9	0.0	99.00	0.0	0.0	0.0	0.475	2.64	-0.641	0.092
10	0.0	99.00	0.0	0.0	0.0	0.475	2.64	-0.791	0.027
11	0.0	99.00	0.0	0.0	0.0	0.475	2.64	-0.617	-0.032
12	0.0	99.00	0.0	0.0	0.0	0.020	1.20	-0.025	-0.002
13	0.0	99.00	0.0	0.0	0.0	0.020	1.20	-0.065	-0.008
14	0.0	99.00	0.0	0.0	0.0	0.020	1.20	-0.029	-0.006
15	0.0	99.00	0.0	0.0	0.0	0.020	0.02	-0.005	-0.002
16	0.0	99.00	0.0	0.0	0.0	0.020	0.02	0.0	-0.001
17	0.0	99.00	0.0	0.0	0.0	0.020	1.20	0.005	-0.003
18	0.0	99.00	0.0	0.0	0.0	0.020	1.20	0.029	-0.003
19	0.0	99.00	0.0	0.0	0.0	0.020	1.20	0.065	-0.002
20	0.0	99.00	0.0	0.0	0.0	0.020	1.20	0.025	0.000
21	0.0	99.00	0.0	0.0	0.0	-0.454	-2.52	0.240	-0.079
22	0.0	99.00	0.0	0.0	0.0	-0.454	-2.52	0.008	-0.220
23	0.0	99.00	0.0	0.0	0.0	-0.454	-2.52	-0.008	-0.216
24	0.0	99.00	0.0	0.0	0.0	0.020	1.20	-0.240	-0.081
25						0.475	2.64	0.0	0.0

X-TWIST = 0.001097573 RAD./IN. — CHECKS. MXX = 7.150 — FXX = 0.0
Y-CURV. = 0.0 RAD./IN. — MXY = 0.0 — FXY = -0.000
Z-CURV. = 0.0 RAD./IN. — MXZ = 0.0 — FXZ = -0.000

OH-58 BRAIDED BLADE — RUN 3 — 4/26/79

CASE 4.17 — LOAD Y = -0.58 — MXX = 0.0 — FXX = 0.0
STA. 90.00 — POINT Z = 0.47 — MXY = 2.600 — FXY = 0.0
MXZ = 0.0 — FXZ = 0.0

NO.	AXIAL STRESS	M.S.	COMPONENTS OF FORCE X	Y	Z	SHEAR FLOW	SHEAR STRESS	SKIN FORCE COMP. Y	Z
1	-1.43	68.93	-0.335	-0.003	-0.000	-0.000	-0.00	-0.000	0.000
2	-1.46	67.30	-0.439	0.0	-0.000	0.000	0.00	-0.000	0.000
3	-1.42	69.57	-0.345	0.002	-0.000	0.000	0.00	0.000	0.000
4	-1.23	80.27	-0.297	0.002	0.000	0.001	0.00	0.000	0.000
5	-1.61	60.98	-0.403	0.003	-0.000	0.001	0.00	0.0	0.000
6	-0.29	99.00	-0.055	0.000	0.000	0.001	0.00	-0.000	0.000
7	1.05	94.43	0.261	-0.002	-0.000	0.001	0.00	-0.001	0.000
8	0.92	99.00	0.225	-0.002	0.000	0.001	0.00	-0.001	0.000
9	1.53	64.30	0.377	-0.003	-0.000	0.000	0.00	-0.001	0.000
10	1.97	49.82	0.591	0.0	-0.001	-0.000	-0.00	0.000	0.000
11	1.94	50.49	0.455	0.004	-0.000	0.000	0.00	-0.000	-0.000
12	1.76	55.96	0.038	0.000	-0.000	0.000	0.00	-0.000	-0.000
13	1.15	85.97	0.045	0.001	-0.000	0.000	0.00	-0.000	-0.000
14	0.33	99.00	0.008	0.000	0.000	-0.000	-0.00	-0.000	0.000
15	0.01	99.00	0.002	0.000	0.000	-0.000	-0.00	0.0	0.000
16	-0.13	99.00	-0.000	-0.000	-0.000	-0.000	-0.00	-0.000	0.000
17	-0.95	99.00	-0.162	-0.002	-0.000	-0.000	-0.00	-0.000	0.000
18	-0.67	99.00	-0.017	-0.000	0.0	-0.000	-0.00	-0.000	0.000
19	-1.04	95.47	-0.140	-0.000	0.0	-0.000	-0.00	-0.000	0.000
20	-1.34	73.39	-0.029	-0.000	-0.000	0.000	0.00	-0.000	0.000
21	-1.23	82.04	-0.108	-0.001	-0.000	0.001	0.00	-0.000	0.000
22	-0.94	99.00	-0.065	-0.001	0.000	0.001	0.00	0.000	0.000
23	1.13	87.46	0.136	0.002	-0.000	0.001	0.00	0.000	0.000
24	1.74	56.36	0.157	0.002	-0.000	0.000	0.01	0.000	0.000
25						-0.001	-0.00	0.0	0.0

X-TWIST = 0.000000342 RAD./IN. — CHECKS. MXX = -0.000 — FXX = 0.000
Y-CURV. = 0.000726264 RAD./IN. — MXY = 2.600 — FXY = 0.000
Z-CURV. = 0.000019271 RAD./IN. — MXZ = -0.000 — FXZ = -0.000

TABLE A-3 (CONTINUED)

4/26/79

OH-58 BRAIDED BLADE — RUN 3

CASE 4.18
STA. 80.00

LOAD Y = -0.58
POINT Z = 0.47

MXX = 0.0 FXX = 32.750
MXY = -1.100 FXY = 0.0
MXZ = 0.0 FXZ = 0.0

NO.	AXIAL STRESS	M.S.	COMPONENTS OF FORCE X	Y	Z	SHEAR FLOW	SHEAR STRESS	SKIN FORCE COMP. Y	Z
1	4.68	20.58	1.095	0.009	0.000	0.000	0.00	-0.000	0.000
2	5.41	17.47	1.624	0.0	0.001	0.002	0.01	0.002	0.000
3	6.28	14.92	1.530	-0.011	0.000	0.003	0.02	0.003	0.000
4	6.99	13.30	1.688	-0.014	-0.000	0.004	0.01	0.002	0.000
5	12.51	7.00	3.124	-0.022	0.001	0.005	0.01	0.001	0.001
6	14.17	6.05	2.805	-0.020	-0.001	0.004	0.01	0.0	0.002
7	15.83	5.32	3.941	-0.027	-0.003	0.003	0.01	-0.001	0.001
8	9.69	9.32	2.358	-0.019	0.000	0.002	0.01	-0.002	0.000
9	9.97	9.03	2.456	-0.017	-0.001	0.001	0.01	-0.002	0.000
10	9.71	9.30	2.920	0.0	-0.004	-0.001	-0.00	-0.000	0.000
11	8.93	10.23	2.086	0.017	-0.002	-0.002	-0.01	0.002	0.000
12	7.43	12.46	0.160	0.002	-0.000	-0.001	-0.05	0.001	0.000
13	5.75	16.39	0.225	0.003	-0.000	-0.001	-0.06	0.002	0.000
14	3.71	25.64	0.093	0.001	0.000	-0.001	-0.06	0.001	0.000
15	11.58	7.65	1.965	0.024	0.000	-0.000	-0.00	0.000	0.000
16	2.93	33.14	0.000	0.000	0.000	-0.000	-0.00	0.0	0.000
17	10.35	8.66	1.760	0.021	0.000	0.001	0.05	0.000	-0.000
18	2.46	39.70	0.061	0.001	0.0	0.001	0.05	0.001	-0.000
19	3.01	32.22	0.116	0.001	0.0	0.001	0.06	0.002	-0.000
20	3.55	27.18	0.076	0.001	0.000	0.001	0.07	0.001	0.000
21	4.51	21.21	0.405	0.005	0.000	0.002	0.01	-0.000	0.000
22	5.31	17.82	0.637	0.008	-0.000	0.002	0.01	-0.000	0.001
23	7.41	12.50	0.889	0.011	-0.000	0.002	0.01	0.000	0.001
24	8.19	11.20	0.737	0.009	-0.000	-0.001	-0.04	0.001	0.000
25						-0.001	-0.00	0.0	0.0

X-TWIST = 0.000101446 RAD./IN.
Y-CURV. = 0.000397374 RAD./IN.
Z-CURV. = -0.000141123 RAD./IN.

CHECKS. MXX = -0.000 FXX = 32.750
MXY = -1.100 FXY = 0.000
MXZ = 0.000 FXZ = -0.000

4/26/79

OH-58 BRAIDED BLADE — RUN 3

CASE 4.20
STA. 80.00

LOAD Y = -0.58
POINT Z = 0.47

MXX = 0.0 FXX = 66.220
MXY = -6.750 FXY = 0.360
MXZ = 0.0 FXZ = 0.0

NO.	AXIAL STRESS	M.S.	COMPONENTS OF FORCE X	Y	Z	SHEAR FLOW	SHEAR STRESS	SKIN FORCE COMP. Y	Z
1	11.95	7.37	2.797	0.023	0.001	0.020	0.11	0.025	-0.001
2	13.50	6.41	4.049	0.0	0.002	0.020	0.11	0.033	0.001
3	15.17	5.59	3.694	-0.026	0.001	0.017	0.10	0.025	0.001
4	16.28	5.14	3.930	-0.032	-0.000	0.014	0.02	0.012	0.002
5	29.08	2.56	7.019	-0.049	0.002	0.007	0.01	0.004	0.002
6	27.14	2.43	5.766	-0.040	-0.001	0.001	0.00	0.0	0.001
7	31.19	2.31	7.514	-0.052	-0.006	-0.007	-0.01	0.002	-0.000
8	17.97	4.56	4.376	-0.035	0.001	-0.012	-0.07	0.008	-0.002
9	17.53	4.71	4.309	-0.030	-0.002	-0.016	-0.09	0.020	-0.003
10	15.21	5.17	4.474	0.0	-0.006	-0.019	-0.11	0.030	-0.001
11	14.62	5.84	3.425	0.029	-0.003	-0.020	-0.11	0.025	0.001
12	11.97	7.35	0.258	0.003	-0.000	-0.018	-1.06	0.022	0.002
13	9.62	9.39	0.376	0.005	-0.000	-0.018	-1.03	0.040	0.007
14	6.93	13.43	0.173	0.002	0.000	-0.017	-1.00	0.025	0.005
15	23.35	3.28	3.970	0.048	0.001	-0.000	-0.00	0.004	0.001
16	5.14	15.20	0.000	0.000	0.000	-0.000	-0.00	0.0	0.000
17	22.54	3.43	3.840	0.047	0.001	0.017	1.00	0.004	-0.002
18	6.14	15.29	0.152	0.002	0.0	0.018	1.03	0.025	-0.003
19	7.89	11.67	0.305	0.004	0.0	0.018	1.07	0.041	-0.002
20	9.52	9.51	0.205	0.003	0.000	0.018	1.09	0.023	0.000
21	11.21	7.93	1.007	0.013	0.000	0.001	0.00	0.012	0.001
22	11.69	7.56	1.303	0.017	-0.000	0.002	0.01	-0.000	0.001
23	13.01	6.68	1.562	0.019	-0.001	0.002	0.01	0.000	0.001
24	13.53	6.39	1.217	0.015	-0.001	-0.018	-1.06	0.013	0.000
25						0.019	0.10	0.0	0.0

X-TWIST = 0.000002329 RAD./IN.
Y-CURV. = 0.000630622 RAD./IN.
Z-CURV. = -0.000308449 RAD./IN.

CHECKS. MXX = 0.000 FXX = 66.220
MXY = -6.750 FXY = 0.360
MXZ = 0.000 FXZ = 0.000

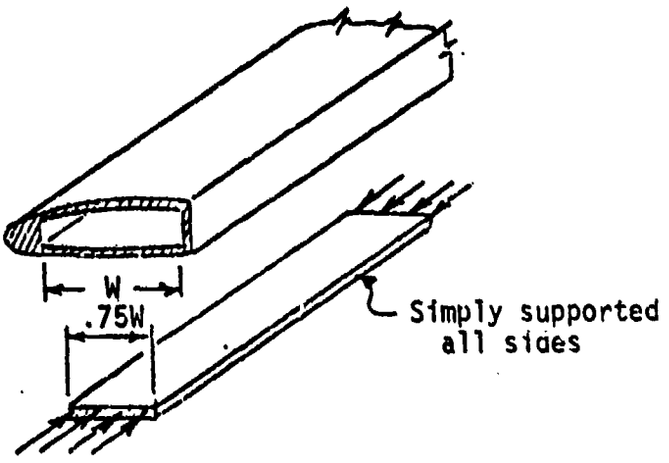

Figure A-13. Plate Idealization for Buckling Analysis.

Reference 14 provides the following formula for the critical buckling stress.

$$\sigma^{cr} = -\frac{1}{t}\left[\frac{(D_{11}D_{22})^{\frac{1}{2}} K_o}{b^2} + \frac{C\pi^2 D_o}{b^2}\right]$$

For the laminate at station 80, Table A-2 gives:

$t = .180$

$D_{11} = 2.132$

$D_{12} = 1.104$

$D_{22} = 1.424$

$D_{33} = 1.117$

$D_o = D_{12} + 2\,D_{33} = 3.338$

From Reference 6, for a long plate simply supported:

$K_o = 19.7$

$C = 2$

From the y coordinates for elements 4 and 21 in Table A3,

$W = 5.3$

$b = .75W = 3.975$

Then,

$$\sigma^{cr} = -\frac{1}{.18}\left|\frac{(2.132 \times 1.424)^{\frac{1}{2}}(19.7)}{(3.975)^2} + \frac{2\pi^2(3.338)}{(3.975)^2}\right| = -35.2 \text{ ksi}$$

$$\text{Buckling, M.S.} = \frac{-35.2}{-9.97} = \underline{+2.53}$$

4. Maximum Shear in Upper and Lower Surface, Case 4.16

From Table A-3, the maximum shear stress = 2.64 ksi for skin elements of the upper and lower surfaces of the spar. From Table A-2, the allowable shear stress - 14.83 ksi.

$$\text{M.S.} = \frac{14.87}{2.64} - 1 = \underline{+4.62} \text{ (ult)}$$

5. Alternating Stresses in Upper and Lower Surfaces, Case 4.17

From Table A-3, the maximum alternating stresses are:

± 1.46 ksi at element 2

± 1.97 ksi at element 10

6. Mean Stress in Upper and Lower Surfaces, Case 4.18

From Table A-3, the corresponding mean stresses are:

5.41 ksi at element 2

9.71 ksi at element 10

Figure A-14 shows a graphical representation of the fatigue margin of safety in the presence of both alternating and mean stresses.

For the Upper Surface, Element 11.

$$\text{M.S.} = \frac{25.52}{9.91} - 1 = \underline{+1.57}$$

For the Lower Surface, Element 2.

$$\text{M.S.} = \frac{23.06}{5.60} - 1 = \underline{+3.12}$$

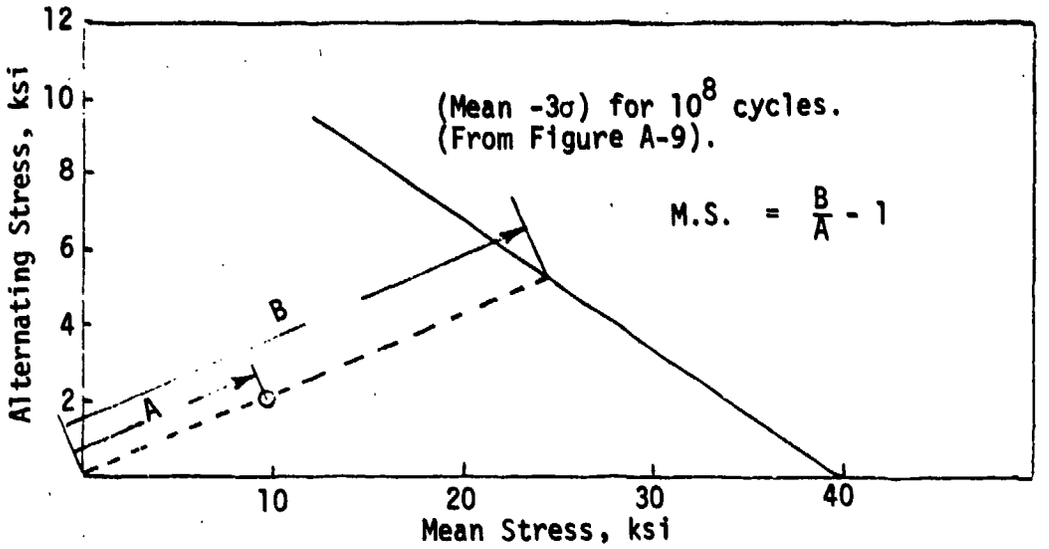

Figure A-14. Graphical Representation of Fatigue Margin of Safety.

APPENDIX B

PROCESS SPECIFICATION

1 SCOPE

1.1 This specification establishes requirements for structures or components of aramid fiber in a cured epoxy matrix having the fiber laydown accomplished predominately by mechanical braiding.

2 APPLICABLE DOCUMENTS

2.1 The following documents of the exact issue stated, form a part of this specification to the extent specified herein.

American Society for Testing Materials (ASTM) Standards

ASTM D 445-74 Kinematic Viscosity of Transparent and Opaque Liquids (and the Calculation of Dynamic Viscosity), Test for

ASTM D 1652-73 Epoxy Content of Epoxy Resins, Test for

ASTM D 2076-64 Acid Value and Amine Value of Fatty Quarternary Ammonium Chlorides, Tests for

ASTM D 2734-70 Void Content of Reinforced Plastics, Test for

ASTM D 3171-73 Fiber Content of Reinforced Resin Composites, Test for

2.2 The following documents of the issue specified by contract or purchase order, form a part of this specification to the extent specified herein.

Kaman Specifications

KPS 190 Adhesive Bonding, Structural

KPS 375 Preparation of Surfaces Prior to Adhesive Bonding

3 REQUIREMENTS

3.1 Equipment and Facilities

3.1.1 Braiding machines shall be capable of producing a closed woven pattern at controlled fiber angle onto the braided structure.

REV.

3.1.2 Scales for weighing resin system shall be accurate within ± 0.2%.

3.1.3 Fabrication area(s) shall be clean, enclosed, separate from other shop operations and environmentally controlled at a temperature of 80°F maximum and a relative humidity of 60% maximum. Temperature and humidity shall be continuously recorded.

3.2 Material

3.2.1 Resin System Components shall comply with Table I and shall be stored at room temperature in sealed containers. Each batch of resin and curing agent shall be retested for conformance to Table I every six months after receipt when in use.

3.2.2 Film adhesives and primers shall be as specified by the Engineering drawing, and shall be stored and handled in accordance with KPS 190.

3.2.3 Yarn, roving and fabric shall be as specified by the Engineering drawing and shall be stored in a clean dry area suitably packaged to prevent contamination. When opened for use these materials shall be kept within an environmentally controlled area conforming to 3.1.3.

TABLE I. MATERIAL REQUIREMENTS

Property	XB-2793[1] Resin	XU 205[1] Curing Agent	Test Method
Dynamic Viscosity (cps)	1500-3500	2000-5000	ASTM D 445
Epoxy Equivalent (WPE)	137-147	---	ASTM D 1652
Amine Value	---	9.9-12.5	ASTM D 2076
Appearance	Clear Pale Yellow	Clear Red	Visual

[1]Manufactured by Ciba-Geigy Corp.

3.3 Procedures

3.3.1 Tool/Process Definition and Preproduction Approval. Tooling and processes employed shall be fully defined and approved before parts for production use are accepted.

3.3.1.1 Tools shall be defined by tool drawings which shall be updated to incorporate any changes made during process development.

3.3.1.2 Work instructions shall be prepared for each assembly design which fully define the processing steps and sequences, and inspections necessary to comply with procedures outlined below and produce consistently acceptable parts. These instructions shall be adequately detailed to preclude inadvertent or uncontrolled process changes which could adversely affect part integrity.

3.3.1.3 An assembly log, which shall be integral with the work instructions or cross referenced thereto, shall be completed for each individual unit. This log shall provide a record of the manufacturer's lot numbers of adhesives, primers, prepregs, glass fabric and roving used, a record of the mix batches of resin used which is traceable to the resin system component manufacturer's lot numbers (see 3.3.3), a record of time between cleaning, priming and curing in those cases where limitations are established, a record of manufacturing or inspection approvals of in-process operations as required by the work instructions, and shall incorporate or provide traceability to the cure cycle and process control test records.

3.3.1.4 Preproduction approval shall require the concurrence of Kaman Materials Engineering and shall be based on nondestructive and destructive examination of at least one assembly and evaluation of the adequacy of the work instuctions, assembly log, and tools. Any tool or process changes shall require reapproval.

3.3.2 Surface Preparation. The surfaces of all cured plastic, metal or other detail parts to be bonded or laminated within the braided assembly shall be prepared in accordance with KPS 375. Adhesive primer, adhesive, or laminating result shall be applied to all bonding surfaces within the time limitations established therein.

3.3.2.1 Primer application, when required by the engineering drawing, and storage life of primed details shall be in accordance with KPS 190.

3.3.2.2 Prepared or prepared and primed details shall be handled and protected so as to preclude contamination, and shall be maintained in an area conforming to 3.1.3 until assembled, except as permitted by KPS 190.

3.3.2.3 Detailed procedures for surface preparation and primer application, and for protection to preclude contamination shall be specified in the work instructions.

3.3.3 Mixing. Resin system components shall be mixed in accordance with the following requirements by personnel who have been trained and certified to perform this work. Work instructions shall provide detailed mixing procedures.

3.3.3.1 The epoxy resin and curing agent shall be mixed in the ratio 100 parts by weight resin to 42.5 parts by weight curing agent.

3.3.3.2 Each container of mixed resin shall be labeled to show the resin components and date and time of mixing, and this data shall be transferred to the assembly log for each operation in which it is used. The manufacturer's batch numbers of resin and curing agent, the actual measured weights of components in the mix batch, and teh identity of the certified mixer shall also be entered in the assembly log, or in a separate mix area log traceable from the entries in the assembly log.

3.3.4 Braiding, Assembly and Impregnation. Fiber braiding and installation of fabric plies, subassemblies and detail parts shall be accomplished in strict accordance with the approved work instructions which comply with 3.3.1.2 and the following.

3.3.4.1 Operations shall be carried out in an environment conforming to 3.1.3.

3.3.4.2 Each braided layer shall exhibit a closed woven pattern with fiber orientation as specified by the engineering drawing. A slight gap or spacing between adjacent parallel yarns or rovings is permissible up to a maximum of .030".

3.3.4.3 Individual yarns or rovings may be spliced by tying the ends together while braiding and subsequently cutting out the knot to leave an .060" maximum gap between the cut ends. Such splices are not permissible in surface layers (including inner surfaces), within three inches of any edge (including holes and cutouts) of the finished structure, or within three inches of each other in any layer.

3.3.4.4 Impregnation of the fiber assembly with the mixed resin system shall be accomplished with the application of vacuum to assist in complete impregnation and removal of air. The resin may be heated to a temperature not in excess of 150°F to reduce viscosity.

3.3.4.5 Assemblies and subassemblies may be staged and debulked as necessary to enhance handling characteristics and develop required resin content by application of controlled heat and pressure cycles detailed in the work instructions.

REV.

3.3.5 Curing. Curing shall be performed in accordance with a time, temperature and pressure cycle that is completely defined in the detail work instructions and will consistantly produce components meeting the requirements herein. The cure cycle shall ensure that the entire assembly is cured at 300 ± 10°F for 4 hours minimum.

3.3.5.1 Heating may be supplied by integrally heated tool, autoclave, oven or platen press. Pressure may be applied by autoclave, pressurized diaphragm, platen press, integrally pressurized tool or die closure.

3.3.5.2 Autoclave pressure, pressure applied through fluid-pressurized tool diaphragm, and vacuum applied to the bag if any, shall be that established by qualification and may be varied within the range of +25% and -10% without requalification. Pressure beneath bags vented to atmosphere shall not exceed 2 psi during the cure cycle. External pressure and pressure beneath the bag shall be monitored during cure, and any departures from the qualified cycle recorded and affected assemblies rejected.

3.3.5.3 When pressure is applied by a press or closed mold any change to the dimensions or tolerances of detail parts shall require process requalification.

3.3.5.4 Temperatures shall be continuously recorded by thermocouples located on the tool adjacent to the component, and/or located in holes in the tool near tool-part interfaces. Quantity, location and correlation of the control thermocouples with actual component temperatures shall be established by a qualification temperature survey of the tool during one or more simulated cure cycles using actual parts with thermocouples located at strategic points within the part.

3.3.5.5 Qualified thermocouple locations, cure pressures and other necessary parameters, such as procedures to control the uniformity of heat-up and time of pressure application shall be incorporated in the work instructions.

3.3.6 Subsequent Operations

3.3.6.1 Methods for removal from the curing fixture, extraction of mandrels or cores, and removal of supporting fixtures or similar tooling aids shall be such as to prevent damage to the cured article. Detailed procedures for such operation shall be incorporated in the approved work instructions.

3.4 Finished Part Requirements

3.4.1 Surface Quality. Except as permitted herein or by the Engineering drawing, composite structures shall be free from cracks, dents, wrinkles, gouges, resin puddles, cut fibers or similar defects or discontinuities. Any mold line resin flash shall be removed so as to blend with adjacent surfaces in level and smoothness.

REV.

3.4.2 Internal Quality. The composite structure shall contain the sequence of braided layers and fabric at the fiber orientation specified by the Engineering drawing in a continuous, completely cured epoxy matrix which is free from resin pockets, crushed or broken fibers, voids or delaminations except as permitted below. Fittings, inserts, etc. which are cocured in place shall be completely bonded to the composite resin, with or without an intermediate layer of film adhesive, as specified by the Engineering drawing.

3.4.2.1 Fiber orientation. Unless otherwise specified by the engineering drawing the fiber orientation shall be within $\pm$ 5° of that specified.

3.4.2.2 Fiber content. Unless otherwise specified by the Engineering drawing the fiber content of the composite may range from 50-60% by volume, but shall be controlled within tighter limits as necessary to meet any specified weight and balance requirements.

3.4.2.3 Microporosity. Unless otherwise specified by the Engineering drawing the void content in any area of the composite shall not exceed 4%.

3.4.2.4 Soundness. Voids, disbonds, or delaminations within the composite or between the composite and bonded-in fittings, inserts, etc., shall not exceed the following limitations.

3.4.2.4.1 No single discontinuity shall exceed one inch in the largest dimension or shall have an area exceeding .5 square inches. Discontinuities closer together than the longest dimension of either shall be considered as a single void.

3.4.2.4.2 Voids are not permissible within .125 inches of the edge of the composite or any joint.

4 QUALITY ASSURANCE PROVISIONS

4.1 Responsibility for Inspection. Unless otherwise specified in the contract or purchase order, the supplier is responsible for the performance of all inspection requirements specified herein. Kaman Aerospace reserves the right to perform any of the inspection requirements set forth in this specification as deemed necessary to assure compliance with the prescribed requirements.

4.2 Materials and Process Control

4.2.1 Quality Assurance Program. A documented program shall be provided which insures that all material and process requirements of Section 3, and the detailed procedures for each part developed in accordance therewith and approved per 3.3.1.4 are continuously complied with during fabrication.

4.3 Preproduction Inspection. Preproduction approval per 3.3.1.4 shall require review and approval of the work instructions and destructive and nondestructive inspection for conformance to 3.4 of one or more actual parts produced by the process.

4.3.1 All nondestructive inspections required by 4.4 shall be performed before destructive examination and the results of both correlated.

4.3.2 Destructive examination shall include the following.

4.3.2.1 All joints between the composite and any bonded in inserts, fittings, preused subassemblies, etc. shall be disassembled and inspected for conformance with 3.4.2.4. All discontinuities shall be recorded.

4.3.2.2 Sections shall be cut through typical areas of the composite structures, including any discontinuities indicated by nondestructive inspection, and examined microscopically for conformance with 3.4.2 and 3.4.2.4.

4.4.2.3 Sections shall be cut from areas representing each winding pattern and layer configuration and checked for fiber content per ASTM D 3171 for conformance to 3.4.2.2, void content per ASTM D 2734 for conformance to 3.4.2.3, and fiber orientation for conformance to 3.4.2.1.

4.4 Quality Conformance Inspection

4.4.1 Ultrasonic Inspection. Conformance with the requirements of 3.4.2.4 thru 3.4.2.4.2 shall be determined by ultrasonic irspection of each part. The equipment and methods used shall be capable of detecting known voids .25 inch in diameter fabricated in reference panels duplicating all sections and laminae of the part tested. Ultrasonic techniques, including equipment, equipment settings, and areas to be inspected with each technique, shall be described in detailed written instructions used in setting up and performing the inspection. These instructions shall require standardization against reference panels whenever setting up to perform a given technique and rechecking against reference panels at least upon completion of inspection.

4.4.1.1 Ultrasonic or inspection techniques shall be correlated with destructive tests of bonded assemblies (see 4.3), and modified as necessary, in order to assure that the best practical detection and delineation of voids and unbonds is achieved.

4.4.2 Radiographic Inspection. Radiographic inspection shall be used as necessary to supplement ultrasonic inspection as required by Kaman Quality Control. Radiographic techniques, including areas to be inspected and all radiographic parameters, shall be described in detailed inspection instructions used in setting up and performing the inspection.

4.4.2.1 Radiographic inspection techniques shall be correlated with destructive tests of bonded assemblies (see 4.3), and modified as necessary, to achieve adequate inspection.

4.4.3 Visual Inspection. Each assembly shall be visually inspected for conformance with 3.4.1.

4.4.4 Weight and Balance Inspection. Each part shall be weighed for conformance to the requirements of the engineering drawing. If the drawing establishes requirements for center of gravity location or moments about specific points, each part shall be inspected for conformance thereto.

DISTRIBUTION LIST

No. of Copies	To
	Commander, U.S. Army Aviation Research and Development Command, 4300 Goodfellow Boulevard, St. Louis, Missouri 63210
10	ATTN: DRDAV-EGX
1	DRDAV-D
1	DRDAV-N
	Project Manager, Advanced Attack Helicopter, P.O. Box 209, St. Louis, Missouri 63166
2	ATTN: DRCPM-AAH-TM
1	DRCPM-AAH-TP
	Project Manager, Black Hawk, P.O. Box 209, St. Louis, Missouri 63166
2	ATTN: DRCPM-BH-T
	Project Manager, CH-47 Modernization, P.O. Box 209, St. Louis, Missouri 63166
2	ATTN: DRCPM-CH-47-MT
	Project Manager, Aircraft Survivability Equipment, P.O. Box 209, St. Louis, Missouri 63166
2	ATTN: DRCPM-ASE-TM
	Project Manager, Cobra, P.O. Box 209, St. Louis, Missouri 63166
2	ATTN: DRCPM-CO-T
	Project Manager, Advanced Scout Helicopter, P.O. Box 209, St. Louis, Missouri 63166
2	ATTN: DRCPM-ASH
	Project Manager, Navigation/Control Systems, Fort Monmouth, New Jersey 07703
2	ATTN: DRCPM-NC-TM
	Project Manager, Tactical Airborne Remotely Piloted Vehicle/Drone Systems, P.O. Box 209, St. Louis, Missouri 63166
2	ATTN: DRCPM-RPV
	Commander, U.S. Army Materiel Development and Readiness Command, 5001 Eisenhower Avenue, Alexandria, Virginia 22333
1	ATTN: DRCMT
1	DRCPM
	Director, Applied Technology Laboratory, Research and Technology Laboratories (AVRADCOM), Fort Eustis, Virginia 23604
1	ATTN: DAVDL-ATL-ATS
	Director, Research and Technology Laboratories (AVRADCOM), Moffett Field, California 94035
1	ATTN: DAVDL-AL-D
	Director, Langley Directorate, U.S. Army Air Mobility Research and Development Laboratories (AVRADCOM), Hampton, Virginia 23365
1	ATTN: DAVDL-LA, Mail Stop 266

No. of Copies	To
	Commander, U.S. Army Avionics Research and Development Activity, Fort Monmouth, New Jersey 07703
1	ATTN: DAVAA-O
	Director, Lewis Directorate, U.S. Army Air Mobility Research and Development Laboratories, 21000 Brookpark Road, Cleveland, Ohio 44135
1	ATTN: DAVDL-LE
	Director, Army Materials and Mechanics Research Center, Watertown, Massachusetts 02172
2	DRXMR-PL
1	DRXMR-PR
1	DRXMR-PD
1	DRXMR-AP
1	DRXMR-PMT
6	DRXMR-RC, Mr. P. Dehmer
	Director, U.S. Army Industrial Base Engineering Activity, Rock Island Arsenal, Rock Island, Illinois 61299
2	ATTN: DRXIB-MT
	Commander, U.S. Army Troop Support and Aviation Materiel Readiness Command, 4300 Goodfellow Boulevard, St. Louis, Missouri 63120
1	ATTN: DRSTS-PLC
1	DRSTS-ME
1	DRSTS-DIL
	Office of the Under Secretary of Defense for Research and Engineering, The Pentagon, Washington, D.C. 20301
1	ATTN: Dr. L. L. Lehn, Room 3D 1079
12	Commander, Defense Technical Information Center, Cameron Station, Alexandria, Virginia 22314
	Defense Industrial Resources Office, DIRSO, Dwyer Building, Cameron Station, Alexandria, Virginia 22314
1	ATTN: Mr. C. P. Downer
	Headquarters, Department of the Army, Washington, D.C. 20310
1	ATTN: DAMA-CSS, Dr. J. Bryant
1	DAMA-PPP, Mr. R. Vawter
	Director, Defense Advanced Research Projects Agency, 1400 Wilson Boulevard, Arlington, Virginia 22209
1	ATTN: Dr. A. Bement
	Commander, U.S. Army Missile Command, Redstone Arsenal, Alabama 35809
1	ATTN: DRSMI-ET
1	DRSMI-RBLD, Redstone Scientific Information Center
1	DRSMI-NSS

No. of Copies	To
	Commander, U.S. Army Tank-Automotive Research and Development Command, Warren, Michigan 48090
1	ATTN: DRDTA-R
1	DRDTA-RCKM, Dr. J. Chevalier
1	Technical Library
	Commander, U.S. Army Tank-Automotive Materiel Readiness Command, Warren, Michigan 48090
1	ATTN: DRSTA-EB
	Commander, U.S. Army Armament Research and Development Command, Dover, New Jersey 07801
1	ATTN: DRDAR-PML
1	Technical Library
1	Mr. Harry E. Pebly, Jr., PLASTEC, Director
	Commander, U.S. Army Armament Research and Development Command, Watervliet, New York 12189
1	ATTN: DRDAR-LCB-S
1	SARWV-PPI
	Commander, U.S. Army Armament Materiel Readiness Command, Rock Island, Illinois 61299
1	ATTN: DRSAR-IRB
1	DRSAR-IMC
1	Technical Library
	Commander, U.S. Army Foreign Science and Technology Center, 220 7th Street, N.E., Charlottesville, Virginia 22901
1	ATTN: DRXST-SD3
	Commander, U.S. Army Electronics Research and Development Command, Fort Monmouth, New Jersey 07703
1	ATTN: DELET-DS
	Commander, U.S. Army Electronics Research and Development Command, 2800 Powder Mill Road, Adelphi, Maryland 20783
1	ATTN: DRDEL-BC
	Commander, U.S. Army Depot Systems Command, Chambersburg, Pennsylvania 17201
1	ATTN: DRSDS-PMI
	Commander, U.S. Army Test and Evaluation Command, Aberdeen Proving Ground, Maryland 21005
1	ATTN: DRSTE-ME
	Commander, U.S. Army Communications-Electronics Command, Fort Monmouth, New Jersey 07703
1	ATTN: DRSEL-LE-R
1	DRSEL-POD-P

No. of Copies	To
	Director, U.S. Army Ballistic Research Laboratory, Aberdeen Proving Ground, Maryland 21005
1	ATTN: DRDAR-TSB-S (STINFO)
	Chief of Naval Research, Arlington, Virginia 22217
1	ATTN: Code 472
	Headquarters, Naval Material Command, Washington, D.C. 20360
1	ATTN: Code MAT-042M
	Headquarters, Naval Air Systems Command, Washington, D.C. 20361
1	ATTN: Code 5203
	Headquarters, Naval Sea Systems Command, 1941 Jefferson Davis Highway, Arlington, Virginia 22376
1	ATTN: Code 035
	Headquarters, Naval Electronics Systems Command, Washington, D.C. 20360
1	ATTN: Code 504
	Director, Naval Material Command, Industrial Resources Detachment, Building 75-2, Naval Base, Philadelphia, Pennsylvania 19112
1	ATTN: Technical Director
	Commander, U.S. Air Force Wright Aeronautical Laboratories, Wright-Patterson Air Force Base, Ohio 45433
1	ATTN: AFWAL/MLTN
1	AFWAL/MLTM
1	AFWAL/MLTE
1	AFWAL/MLTC
	National Aeronautics and Space Administration, Washington, D.C. 20546
1	ATTN: AFSS-AD, Office of Scientific and Technical Information
	National Aeronautics and Space Administration, Marshall Space Flight Center, Huntsville, Alabama 35812
1	ATTN: R. J. Schwinghammer, EH01, Dir., M&P Lab
1	Mr. W. A. Wilson, EH41, Bldg. 4612
1	Metals and Ceramics Information Center, Battelle Columbus Laboratories, 505 King Avenue, Columbus, Ohio 43201
	Hughes Helicopters-Summa, M/S T-419, Centinella Avenue and Teale Street, Culver City, California 90230
1	ATTN: Mr. R. E. Moore, Bldg. 314
	Sikorsky Aircraft Division, United Aircraft Corporation, Stratford, Connecticut 06497
1	ATTN: Mr. Melvin M. Schwartz, Chief, Manufacturing Technology

No. of Copies	To
	Bell Helicopter Textron, Division of Textron, Inc., P.O. Box 482, Fort Worth, Texas 76101
1	ATTN: Mr. P. Baumgartner, Chief, Manufacturing Technology
	Kaman Aerospace Corporation, Bloomfield, Connecticut 06002
1	ATTN: Mr. A. S. Falcone, Chief, Materials Engineering
	Boeing Vertol Company, Box 16858, Philadelphia, Pennsylvania 19142
1	ATTN: R. Pinckney, Manufacturing Technology
1	R. Drago, Advanced Drive Systems Technology
	Detroit Diesel Allison Division, General Motors Corporation, P.O. Box 894, Indianapolis, Indiana 46206
1	ATTN: James E. Knott, General Manager
	General Electric Company, 10449 St. Charles Rock Road, St. Ann, Missouri 63074
1	ATTN: Mr. H. Franzen
	AVCO-Lycoming Corporation, 550 South Main Street, Stratford, Connecticut 06497
1	ATTN: Mr. V. Strautman, Manager, Process Technology Laboratory
	United Technologies Corporation, Pratt & Whitney Aircraft Division, Manufacturing Research and Development, East Hartford, Connecticut 06108
1	ATTN: Mr. Ray Traynor
	Grumman Aerospace Corporation, Plant 2, Bethpage, New York 11714
1	ATTN: Richard Cyphers, Manager, Manufacturing Technology
1	Albert Grenci, Manufacturing Engineer, Department 231
	Lockheed Missiles and Space Company, Inc., Manufacturing Research, 1111 Lockheed Way, Sunnyvale, California 94088
1	ATTN: H. Dorfman, Research Specialist
	Lockheed Missiles and Space Company, Inc., P.O. Box 504, Sunnyvale, California 94086
1	ATTN: D. M. Schwartz, Dept. 55-10, Bldg. 572

U.S. Army Aviation Research and Development Command, St. Louis, Missouri 63120
DEVELOPMENT OF MANUFACTURING TECHNOLOGY FOR FABRICATION OF A COMPOSITE HELICOPTER MAIN ROTOR SPAR BY TUBULAR BRAIDING - Mark L. White, Kaman Aerospace Corporation, Old Windsor Road, Bloomfield, Connecticut 06002

Technical Report AVRADCOM TR 81-F-9, April 1981, illus-tables, Contract DAAG46-78-C-0070, D/A Project 1767079, AMCMS Code 1497946S7079 (XS6), Final Report, Sep 78 to Sep 80

AD _____

UNCLASSIFIED
UNLIMITED DISTRIBUTION

Key Words

Helicopters
Helicopter rotors
Composite materials
Braiding
Synthetic fibers
Kevlar

Mechanical tubular braiding has been shown to be a viable blade spar manufacturing process in a program which included preliminary design of an improved main rotor blade for the OH-58 helicopter having as its primary structural member a Kevlar 49®/epoxy spar fabricated by braiding. Achievement of an analytically acceptable blade and spar design meeting critical structural and dynamic requirements was not hindered by braiding process constraints. Mechanical property tests of flat panels and spar sections exhibited excellent correlation with analytical predictions. Ballistic testing of spar sections demonstrated superior containment of structural damage. Manufacturing cost estimates predict a price reduction of 1/3 for the braided spar relative to an S-glass/epoxy spar fabricated by orthodox, low-cost technology.

U.S. Army Aviation Research and Development Command, St. Louis, Missouri 3120
DEVELOPMENT OF MANUFACTURING TECHNOLOGY FOR FABRICATION OF A COMPOSITE HELICOPTER MAIN ROTOR SPAR BY TUBULAR BRAIDING - Mark L. White, Kaman Aerospace Corporation, Old Windsor Road, Bloomfield, Connecticut 06002

Technical Report AVRADCOM TR 81-F-9, April 1981, illus-tables, Contract DAAG46-78-C-0070, D/A Project 1767079, AMCMS Code 1497946S7079 (XS6), Final Report, Sep 78 to Sep 80

AD _____

UNCLASSIFIED
UNLIMITED DISTRIBUTION

Key Words

Helicopters
Helicopter rotors
Composite materials
Braiding
Synthetic fibers
Kevlar

Mechanical tubular braiding has been shown to be a viable blade spar manufacturing process in a program which included preliminary design of an improved main rotor blade for the OH-58 helicopter having as its primary structural member a Kevlar 49®/epoxy spar fabricated by braiding. Achievement of an analytically acceptable blade and spar design meeting critical structural and dynamic requirements was not hindered by braiding process constraints. Mechanical property tests of flat panels and spar sections exhibited excellent correlation with analytical predictions. Ballistic testing of spar sections demonstrated superior containment of structural damage. Manufacturing cost estimates predict a price reduction of 1/3 for the braided spar relative to an S-glass/epoxy spar fabricated by orthodox, low-cost technology.

U.S. Army Aviation Research and Development Command, St. Louis, Missouri 63120
DEVELOPMENT OF MANUFACTURING TECHNOLOGY FOR FABRICATION OF A COMPOSITE HELICOPTER MAIN ROTOR SPAR BY TUBULAR BRAIDING - Mark L. White, Kaman Aerospace Corporation, Old Windsor Road, Bloomfield, Connecticut 06002

Technical Report AVRADCOM TR 81-F-9, April 1981, illus-tables, Contract DAAG46-78-C-0070, D/A Project 1767079, AMCMS Code 1497946S7079 (XS6), Final Report, Sep 78 to Sep 80

AD _____

UNCLASSIFIED
UNLIMITED DISTRIBUTION

Key Words

Helicopters
Helicopter rotors
Composite materials
Braiding
Synthetic fibers
Kevlar

Mechanical tubular braiding has been shown to be a viable blade spar manufacturing process in a program which included preliminary design of an improved main rotor blade for the OH-58 helicopter having as its primary structural member a Kevlar 49®/epoxy spar fabricated by braiding. Achievement of an analytically acceptable blade and spar design meeting critical structural and dynamic requirements was not hindered by braiding process constraints. Mechanical property tests of flat panels and spar sections exhibited excellent correlation with analytical predictions. Ballistic testing of spar sections demonstrated superior containment of structural damage. Manufacturing cost estimates predict a price reduction of 1/3 for the braided spar relative to an S-glass/epoxy spar fabricated by orthodox, low-cost technology.

U.S. Army Aviation Research and Development Command, St. Louis, Missouri 63120
DEVELOPMENT OF MANUFACTURING TECHNOLOGY FOR FABRICATION OF A COMPOSITE HELICOPTER MAIN ROTOR SPAR BY TUBULAR BRAIDING - Mark L. White, Kaman Aerospace Corporation, Old Windsor Road, Bloomfield, Connecticut 06002

Technical Report AVRADCOM TR 81-F-9, April 1981, illus-tables, Contract DAAG46-78-C-0070, D/A Project 1767079, AMCMS Code 1497946S7079 (XS6), Final Report, Sep 78 to Sep 80

AD _____

UNCLASSIFIED
UNLIMITED DISTRIBUTION

Key Words

Helicopters
Helicopter rotors
Composite materials
Braiding
Synthetic fibers
Kevlar

Mechanical tubular braiding has been shown to be a viable blade spar manufacturing process in a program which included preliminary design of an improved main rotor blade for the OH-58 helicopter having as its primary structural member a Kevlar 49®/epoxy spar fabricated by braiding. Achievement of an analytically acceptable blade and spar design meeting critical structural and dynamic requirements was not hindered by braiding process constraints. Mechanical property tests of flat panels and spar sections exhibited excellent correlation with analytical predictions. Ballistic testing of spar sections demonstrated superior containment of structural damage. Manufacturing cost estimates predict a price reduction of 1/3 for the braided spar relative to an S-glass/epoxy spar fabricated by orthodox, low-cost technology.